

Dark matter protohalos in MSSM-9 and implications for direct and indirect detection

Roberta Diamanti,¹ Maria Eugenia Cabrera Catalan,^{1,2,3} and Shin'ichiro Ando¹

¹*GRAPPA Institute, University of Amsterdam, 1098 XH Amsterdam, The Netherlands*

²*Instituto de Física, Universidade de São Paulo, São Paulo Brazil*

³*Instituto de Física Teórica, IFT-UAM/CSIC,
U.A.M. Cantoblanco, 28049 Madrid, Spain*

(Dated: February 11, 2022)

We study how the kinetic decoupling of dark matter within a minimal supersymmetric extension of the standard model, by adopting nine independent parameters (MSSM-9), could improve our knowledge of the properties of the dark matter protohalos. We show that the most probable neutralino mass regions, which satisfy the relic density and the Higgs mass constraints, are those with the lightest supersymmetric neutralino mass around 1 TeV and 3 TeV, corresponding to Higgsino-like and Wino-like neutralino, respectively. The kinetic decoupling temperature in the MSSM-9 scenario leads to a most probable protohalo mass in a range of $M_{\text{ph}} \sim 10^{-12} - 10^{-7} M_{\odot}$. The part of the region closer to ~ 2 TeV gives also important contributions from the neutralino-stau co-annihilation, reducing the effective annihilation rate in the early Universe. We also study how the size of the smallest dark matter substructures correlates to experimental signatures, such as the spin-dependent and spin-independent scattering cross sections, relevant for direct detection of dark matter. Improvements on the spin-independent sensitivity might reduce the most probable range of the protohalo mass between $\sim 10^{-9} M_{\odot}$ and $\sim 10^{-7} M_{\odot}$, while the expected spin-dependent sensitivity provides weaker constraints. We show how the boost of the luminosity due to dark matter annihilation increases, depending on the protohalo mass. In the Higgsino case, the protohalo mass is lower than the canonical value often used in the literature ($\sim 10^{-6} M_{\odot}$), while $\langle \sigma v \rangle$ does not deviate from $\langle \sigma v \rangle \sim 10^{-26} \text{ cm}^3 \text{ s}^{-1}$; there is no significant enhancement of the luminosity. On the contrary, in the Wino case, the protohalo mass is even lighter, and $\langle \sigma v \rangle$ is two orders of magnitude larger; as its consequence, we see a substantial enhancement of the luminosity.

I. INTRODUCTION

There is solid evidence that most matter in the Universe is in the form of non-baryonic dark matter (DM) [1–4]. From the theoretical point of view there are several particle physics theories which attempt to explain the yet unknown fundamental nature of DM. In the literature a plethora of DM candidates have been proposed (see, e.g., Ref. [5]). Depending on their masses and interaction cross sections with themselves or ordinary matter, they all exhibit a present day abundance in agreement with the DM density determined by Planck satellite, $\Omega_\chi h^2 = 0.1197 \pm 0.0022$ [6]. Among all particle physics candidates the most popular ones belong to the class of weakly interacting massive particles (WIMPs) [1, 7], since they are assumed to be stable and to have interactions with the standard model (SM) particles, giving a correct relic abundance as observed today.

Although the SM describes the elementary particles and their interactions with great success, there are other good reasons, besides the need of a DM candidate, for expecting physics beyond the SM. One motivation is the so-called *hierarchy problem*. The mass of the Higgs boson acquires large quantum quadratic corrections proportional to the scale where the SM is valid. Assuming the SM is valid up to very high energy scales, the parameters in the theory have to be fine-tuned in order to keep the Higgs mass at an acceptable value of around 126 GeV. Since in the SM a symmetry that relates the various couplings does not exist, this situation is considered to be very unnatural (e.g., Refs. [8–10]). One of the best motivated scenarios introduced to solve this problem is supersymmetry (SUSY), with sparticle masses at the TeV scale. Although the first run of the Large Hadron Collider (LHC) placed important constraints to light sparticles, and a Higgs with 126 GeV shifts the scale of SUSY to larger values requiring a certain amount of tuning (typically at $\mathcal{O}(1\%)$ for the MSSM, see e.g. [11]), SUSY continues being a very attractive possibility.

Another interesting feature of SUSY, mostly related to cosmology and the search for DM, is the existence of a conserved quantum number called R-parity, which assigns at each (super)partner of the SM particles $R = -1$ while each ordinary particle is assigned $R = +1$. This quantum number implies that supersymmetric particles must be created or destroyed in pairs, and that the lightest supersymmetric particle (LSP) is absolutely stable, and hence DM candidates. In many supersymmetric extensions of SM, the lightest neutralino, a linear combination of the superpartners of the neutral gauge and Higgs bosons, is the favoured DM candidate.

With the WIMP hypothesis, the abundance of DM originates from thermal decoupling in the early Universe. When the processes of pair-annihilation and pair-creation of WIMPs go out of chemical equilibrium due to the Hubble expansion, the resulting number density freezes out and remains constant per comoving volume until the present time. This chemical decoupling, however, does not signal the end of WIMP interactions with thermal plasma. There could still be elastic scattering processes with SM particles, which keep WIMPs in kinetic equilibrium until later time. When the rate for elastic scattering processes also falls below the Hubble expansion rate, WIMPs enter the epoch called *kinetic decoupling*. From this point on, WIMPs are decoupled from the thermal bath, and begin to free-stream. After this stage, first gravitationally bound DM structures begin to form, with the size set by the temperature of kinetic decoupling, related to a small-scale cutoff in the primordial power spectrum of density perturbations. Reference [12] calculated the the primordial power spectrum by including collisional damping and free-streaming of WIMPs, and showed that the free-streaming led to a cold DM (CDM) power spectrum with a cutoff around a scale corresponding to the Earth mass, $\sim 10^{-6} M_\odot$ (see also Refs. [13–16]).

One of the most challenging goals today is to shed light on the nature of the small-scale cutoff in the primordial power spectrum of density perturbations, often dubbed with the name of *protohalo*.¹ Its properties are relevant for indirect DM searches. Indirect DM detection looks for signatures

¹ In the following, we use indistinctly “protohalos” or “subhalos” referring to protohalos, which are the smallest possible DM halos.

of DM annihilation, such as gamma-ray photons, from dense celestial environments, where the protohalo mass is a relevant quantity to determine the substructure “boost” factor. Direct detection experiments of DM look for energy deposition in underground detectors caused by scattering interactions between target nuclei and WIMPs around us, giving valuable information about the scattering cross section, and through a correlation that we find in this study, they constrain the mass of the DM protohalos.

Recently, Cornell and Profumo [17] studied scattering cross sections that are relevant for direct detection experiments and protohalo sizes in an MSSM context for the neutralino DM. They based their MSSM scan on 9 parameters defined at the electroweak scale. They found a strong correlation between the kinetic decoupling temperature and the spin-dependent (SD) cross section of neutralinos off nucleons. On the contrary, a weaker correlation was found in the case of the spin-independent (SI) neutralino-nucleon cross section.

In the present paper, we do a forecast on the mass of the protohalos within a supersymmetric scenario by taking into account the latest data from all the relevant particle physics experiments as well as the relic density constraints. We perform our analyses within a Bayesian framework, by adopting 10 MSSM fundamental parameters defined at the gauge couplings unification scale, among which 9 of them we allow to vary after requiring the correct electroweak symmetry breaking.

In the considered MSSM scenario, we find that the kinetic decoupling temperature leads to the protohalo mass most probably residing in a range of $M_{\text{ph}} \sim 10^{-12} - 10^{-7} M_{\odot}$. This large variation is due to the range of the kinetic decoupling temperature, T_{kd} , since in the neutralino annihilation processes, both gauge bosons and fermions play a role, and these couplings reveal to be independent from one another. The range corresponds to two most probable posterior regions: Higgsino-like and Wino-like neutralinos, for which the most probable neutralino masses are around 1 TeV and 3 TeV, respectively.

In these most probable cases, we find that protohalo mass correlates with the both SD and SI scattering cross sections. We show that all Higgsino-like neutralino regions, where the probability is higher, such a scattering is dominantly spin-dependent. Therefore, any experimental measurement of the SD cross section will imply direct consequences on minimal protohalo mass.²

We also show how future direct and indirect detection experiments can play an important role in constraining the (most probable) minimal protohalo mass down to $\sim 10^{-9} M_{\odot}$ and the expected value of the boost of the luminosity due to the annihilation of DM in those regions. Complementarity, we study how those predictions change in regions that are disfavored by the posterior probability density function (PDF) due to the large tuning, necessary to reproduce the experimental observables (including M_Z).

This paper is organized as follows. We describe the supersymmetric model we adopt in Sec. II. The role of the DM protohalo is discussed in Sec. III: A brief explanation of the smallest DM protohalo mass in Sec. III A. The discussion of the most probable regions of the MSSM and interactions involved in the annihilation of neutralinos are presented in Sec. III B. A profile likelihood map is discussed in Sec. III C. We comment on the impact of the direct detection experiments on the mass of the protohalo in Sec. IV, and estimate of the boost of the luminosity due to the annihilation rate in a DM halo with substructures in Sec. V. We finally give our conclusions in Sec. VI.

II. THE MINIMAL SUPERSYMMETRIC STANDARD MODEL AFTER THE FIRST RUN OF THE LHC

Despite the expectation around a potential discovery of light SUSY particles at the first run of the LHC, so far no signal of new physics has been found, which could be considered in tension with

² This is true if the scattering is mediated by a Z boson. The scattering could also be mediated by sleptons; in this case, we do not see such a correlation.

the ideas of natural SUSY. However, the relative large mass of the Higgs boson points to a heavier mass spectrum, suggesting that the lack of discovery of sparticles in the first run of the LHC is a consequence of the Higgs mass value.

In the MSSM, a lightest Higgs boson of around 126 GeV implies a range of M_{SUSY} between $\sim 10^3$ GeV and $\sim 3 \cdot 10^4$ GeV,³ where M_{SUSY} represents the scale at which SUSY particles decouple from the SM (for details, see [18, 19]). Hence, within the MSSM framework the Higgs mass is in tension with naturalness of the electroweak symmetry breaking, requiring a typical tuning of $\mathcal{O}(1)\%$, see, e.g., [11]. This tension is relaxed going beyond the MSSM [20–24]. Moreover, since stops give the most important contribution to the Higgs mass, the allowed range of M_{SUSY} could be written as a constraint to the stop sector, where typically stop masses should be larger than ~ 3 TeV, unless its mixing parameter reaches its maximal value [25], leaving basically the rest of the SUSY spectrum unconstrained.⁴

On the other hand, one of the beautiful aspects of SUSY is the apparent unification of gauge couplings in the MSSM, because it gives a strong hint in favor of grand unified theories suggesting, as well, that we know how the renormalization group equations (RGE) behave up to the gauge coupling unification scale, M_{GUT} .⁵ Taking SUSY parameters at M_{GUT} leads to implicit relations between sparticle masses, in particular the average of stop masses at the scale of 1 TeV for $\tan \beta = 10$, $\bar{m}_{t_{1,2}}^2$, written as a function of the soft parameters at M_{GUT} reads, [11]:

$$\begin{aligned} \bar{m}_{t_{1,2}}^2 \simeq & (2.972 M_3^2 + 0.339 m_{\tilde{Q}_3}^2 + 0.305 m_{\tilde{U}_3}^2 + 0.091 M_2^2 - 0.154 m_{H_u}^2 - 0.052 A_t^2 \\ & + 0.017 M_1^2 \dots) + m_t^2, \end{aligned} \quad (1)$$

where M_1 , M_2 and M_3 are the bino, wino and gluinos soft mass terms, respectively, $m_{\tilde{Q}_3}$ and $m_{\tilde{U}_3}$ are the third generation of squark soft masses, and m_{H_u} is the H_u soft mass. Equation (1) shows that large stop masses imply large gluino mass ($M_{\tilde{g}} \simeq 2.22 M_3$), unless the soft mass terms of the third generation squarks are very large, which leads to a scenario like split SUSY [27].

Regarding naturalness, the largest tuning required to get the correct electroweak symmetry breaking is applied on the μ parameter. From the minimization of the Higgs potential one obtains

$$\begin{aligned} \frac{1}{2} M_Z^2 = & (1.62 M_3^2 - 0.64 m_{H_u}^2 + 0.37 m_{\tilde{Q}_3}^2 + 0.29 m_{\tilde{U}_3}^2 - 0.29 A_t M_3 - 0.20 M_2^2 \\ & + 0.14 M_2 M_3 + 0.11 A_t^2 + \dots) - \mu^2, \end{aligned} \quad (2)$$

where this expression is valid at a scale of 1 TeV for $\tan \beta = 10$ [11]. As in Eq. (1), M_3 is the responsible for the larger contribution. The current gluino mass bound from ATLAS and CMS [28, 29], $m_{\tilde{g}} > 1.33$ TeV (assuming 100% decay to $q\bar{q}\chi_1^0$ and a mass difference between \tilde{g} and χ_1^0 of at least 200 GeV), is that more stringent for naturalness. From Eqs. (1) and (2), we could also see that naturalness and Higgs constraints affect mainly the gluino and squarks sector. On the other hand, sleptons, Binos and Winos are basically unconstrained.

In a more general framework, where the MSSM is parameterized at EW symmetry breaking scale, the pMSSM, the Higgs mass measurements constrain mainly the stop sector, leaving the rest of the spectrum effectively unconstrained. In this case, the main constraints for sparticle masses come from LHC limits and B-physics (see, e.g., Refs. [30–33]).

³ This range is valid for relatively large values of $\tan \beta$.

⁴ Notice that Ref. [11] re-examined the natural SUSY scenarios, and showed that light stop masses (closer to its lower limit after imposing the Higgs mass) are not really a generic requirement of natural SUSY scenarios.

⁵ In gravity, mediated SUSY breaking scenarios conditions are set at M_{Plank} . A popular approximation is to start the RGE running from M_{GUT} instead of M_{Plank} . For some particular scenarios, this approximation is not necessarily correct [26].

Besides the tuning associated to the EW symmetry breaking, there is also a tuning associated to the requirement of having a good DM candidate. Refs [34, 35] study the fine tuning required to obtain the correct DM relic density. In particular, [35] shows that the region of 1 TeV, corresponding to the lightest Higgsino-like neutralino, requires very smallest tuning. Typically, regions where the correct annihilation cross section is dominated by resonances or sfermion-neutralino co-annihilations require a large tuning.

To study the MSSM parameter space we perform a Bayesian analysis. One of the interesting aspects of this approach is that it is possible to take into account naturalness arguments [36]. A fine-tuning associated to the electroweak symmetry breaking is included when we takes the mass of the Z boson in the same foot as rest of the experimental data. Effectively, after requiring the correct electroweak symmetry breaking, the posterior PDF appears to be proportional to a term that penalizes regions with a large fine-tuning, independently of the choice of the prior probability. Interestingly, this term is inversely proportional to the Barbieri-Giudice fine-tuning parameter [37]. More specifically the EW fine tuning penalization appears as a Jacobian factor that arise from the change of variables $\{g_i, y_i, \mu, B\} \rightarrow \{\alpha_i, m_f, M_Z, \tan \beta\}$ evaluated at the measured value of M_Z , where g_i and y_i are the gauge and Yukawa couplings respectively, B is the bilinear Higgs coupling, and μ is the Higgs mass term in the superpotential defined at the SUSY breaking scale. This Jacobian factor is completely independent of the choice of parameters and is not based in a specific definition of fine-tuning. In the same way, a fine-tuning penalization associated to all the other experimental observables is included. Motivated by the fact that this definition does not involve prejudices, Ref. [38] came up with the idea of using this covariant matrix to penalize regions with large fine-tuning in a χ^2 analysis.

In our analysis we assume gravity mediated SUSY breaking and parameterize the MSSM with 10 fundamental parameters defined at the unification scale of the gauge couplings as well as SM parameters. We also assume unification and universality conditions for the squark masses, slepton masses and trilinear terms. The set of 10 parameters is:

$$\{g_i, y_i, M_1, M_2, M_3, m_0^{sq}, m_0^{sl}, m_H, A_0^{sq}, A_0^{sl}, \mu, B\}, \quad (3)$$

where we added, as well, the gauge and Yukawa couplings, g_i and y_i , respectively. M_1, M_2, M_3 are the gaugino masses, m_0^{sq}, m_0^{sl} and m_H are the soft squark, slepton and Higgs masses, A_0^{sq} and A_0^{sl} are the squarks and slepton trilinear couplings, B is the bilinear Higgs coupling, and μ is the Higgs mass term in the superpotential.

Using a more convenient parameterization, the effective set of parameters reads:

$$\{s, M_1, M_2, M_3, m_0^{sq}, m_0^{sl}, m_H, A_0^{sq}, A_0^{sl}, \tan \beta, \text{sign}(\mu)\}, \quad (4)$$

where s stands for SM parameters described in Table I and, without loss of generality, the sign of μ is fixed to +1, allowing M_i to have positive and negative values. In such a way we cover regions with relative phases between μ and M_i .

Let us comment about how strong the predictions of the scenario we consider are with respect to the most general MSSM. In our approach we assume that SUSY was broken at gauge-coupling unification scale. Although this assumption is reasonable in gravity-mediated SUSY breaking scenarios, it is not the only possibility; for example, in gauge mediated scenarios it can happen in principle at any scale. Moreover, the consequence of this assumption depends on the freedom we give to the soft parameters. Imposing universality condition (squark and slepton squared-mass matrices proportional to the 3×3 identity matrix) and unification condition (right sfermion masses equal to left sfermion masses and $m_{H_u} = m_{H_d}$) implies a specific mass hierarchy for squarks and sleptons which could be ameliorated if the SUSY breaking scale is smaller. Hence, the regions

	Gaussian prior	Range scanned	ref.
M_t [GeV]	173.2 ± 0.9	(167.0, 178.2)	[42]
$m_b(m_b)^{\tilde{M}S}$ [GeV]	4.20 ± 0.07	(3.92, 4.48)	[43]
$[\alpha_{em}(M_Z)^{\tilde{M}S}]^{-1}$	127.955 ± 0.030	(127.835, 128.075)	[43]
$\alpha_s(M_Z)^{\tilde{M}S}$	0.1176 ± 0.0020	(0.1096, 0.1256)	[44]

TABLE I. Nuisance parameters adopted in the scan.

of parameters we are missing in using this parameterization of the MSSM are the ones with any possible hierarchies of sfermions masses. In our case, \tilde{t}_1 is always the lightest stop and $\tilde{\tau}_1$ the lightest slepton. On the other hand, the universality condition is supported by the strong constraints from FCNC process.

Using a more general parameterization at EW symmetry breaking scale, the pMSSM, the sparticle masses do not feel the impact of the renormalization group equations,⁶ the correlation between the parameters disappear and the choice of the prior will most likely dominates the results not allowing us to make conclusions about the most probable region. On the other hand, Bayesian analysis has been performed in the pMSSM from different perspectives, to be able to identify which are the parameters that are directly constrained by the experimental information, that can be checked by looking at the prior dependency in each parameter (see, e.g., Refs. [39–41]).

To perform the analysis, we follow the lines described in Ref. [45], where two different priors are considered: standard log priors (S-log prior), which takes a log prior for each parameter independently, and improved log priors (I-log prior), which assumes a common origin for the soft-masses, as expected from SUSY breaking mechanisms. The range of the parameters in our scan varies from 10 GeV to 10^6 GeV. Although both of the considered priors are based on logarithmic space, they are quite different from one another; S-log prior, for example, favors large splittings between the parameters, while I-log priors assume a common origin for the soft parameters. For a more detailed discussion about the priors see Sec. 3.3 of Ref. [45]. Notice that following this approach, which takes naturalness arguments into account, we are able to explore a large range of the parameters and get a consistent result. Previous Bayesian analyses followed a different approach finding prior dependency in their results, showing that not including M_Z as a experimental observable, and therefore not taking into account EW fine-tuning, it is not possible to conclude about the most probable region, for example in the CMSSM.

The experimental data considered in our analysis is described in Table II, where we include electroweak precision measurements [46], B-physics observables [47–51],⁷ the Higgs mass [56, 57], and constraints on the WIMP-nucleon scattering cross-section by XENON-100 [58]. In addition, we include the measured relic density according to *Planck* results [59] because we assume a scenario with a single DM component which is produced thermally in the early Universe.⁸

For the numerical analysis we use **SuperBayeS-v2.0**, a publicly available package that include **MultiNest** [67, 68] nested sampling algorithm, **Softsusy** [69] for the computation of the mass spectrum, **micrOmegas** [70] for the computation of the relic density, **DarkSusy** [71] for the computation of direct⁹ and indirect detection observable, **SusyBSG** [73] and **Superiso** [74] for B-physics observable.

⁶ However, the universality condition is somehow taken into account in the pMSSM, when setting first and second generation sfermion masses equal.

⁷ The updated values for B decays are, for example, $\text{BR}(\bar{B} \rightarrow s\gamma) = (3.43 \pm 0.22 \pm 0.07) \times 10^{-4}$ [52] (see also Refs. [53, 54]) and $\text{BR}(\bar{B} \rightarrow \mu^+\mu^-) = 2.8_{-0.6}^{+0.7} \times 10^{-9}$ [55]. All these measurements are still in agreement (within uncertainties) with the values that we adopted in our analysis, and therefore, their impact would not be large.

⁸ In our analysis, we assume that 100% of dark matter consists of the neutralino. If there is other dark matter components, we need to regard the measurement of the dark matter density determined by Planck satellite as an upper limit, and follow some scaling ansatz studied in, e.g., [45, 60]. This is however beyond the scope of this paper.

⁹ For the contribution of the light quarks to the nucleon form factors, concerning the spin-independent WIMP-nucleon cross section, we have adopted the values $f_{Tu} = 0.02698$, $f_{Td} = 0.03906$ and $f_{Ts} = 0.36$ [72], derived experimentally from measurements of the pion-nucleon sigma term.

Observable	Mean value		Uncertainties		Ref.
	μ	σ (exper.)	τ (theor.)		
M_W [GeV]	80.399	0.023	0.015		[61]
$\sin^2 \theta_{eff}$	0.23153	0.00016	0.00015		[61]
$\text{BR}(\bar{B} \rightarrow X_s \gamma) \times 10^4$	3.55	0.26	0.30		[62]
$R_{\Delta M_{B_s}}$	1.04	0.11	-		[48]
$\frac{\text{BR}(\bar{B}_u \rightarrow \tau \nu)}{\text{BR}(\bar{B}_u \rightarrow \tau \nu)_{SM}}$	1.63	0.54	-		[62]
$\Delta_{0-} \times 10^2$	3.1	2.3	-		[63]
$\frac{\text{BR}(B \rightarrow D \tau \nu)}{\text{BR}(B \rightarrow D e \nu)} \times 10^2$	41.6	12.8	3.5		[49]
R_{l23}	0.999	0.007	-		[50]
$\text{BR}(D_s \rightarrow \tau \nu) \times 10^2$	5.38	0.32	0.2		[62]
$\text{BR}(D_s \rightarrow \mu \nu) \times 10^3$	5.81	0.43	0.2		[62]
$\text{BR}(D \rightarrow \mu \nu) \times 10^4$	3.82	0.33	0.2		[62]
$\Omega_\chi h^2$	0.1196	0.0031	0.012		[64]
m_h [GeV]	125.66	0.41	2.0		[42]
$\text{BR}(\bar{B}_s \rightarrow \mu^+ \mu^-)$	3.2×10^{-9}	1.5×10^{-9}	10%		[51]
	Limit (95% CL)		τ (theor.)		Ref.
Sparticle masses	As in Table 4 of Ref. [65].				
$m_\chi - \sigma_{\chi N}^{\text{SI}}$	XENON100 2012 limits (224.6×34 kg days)				[66]

TABLE II. Observables used for the computation of the likelihood function. For each quantity we use a likelihood function with mean μ and standard deviation $s = \sqrt{\sigma^2 + \tau^2}$, where σ is the experimental uncertainty and τ represents our estimate of the theoretical uncertainty. Lower part: observables for which, at the moment, only limits exist. The explicit form of the likelihood function is given in ref. [65]. In particular, in order to include an appropriate theoretical uncertainty in the observables, the likelihood contains a smearing out of experimental errors and limits.

For the Wino-like and Higgsino-like LSP cases, the Sommerfeld enhancement¹⁰ of the primordial and present day neutralino annihilation has been included, following the lines of Refs. [77–80], using **DarkSE** [81, 82], which is a package for **DarkSusy**. We created a grid in the M_2 – μ plane and performed interpolations to correct the values of the relic density and the present day neutralino annihilation within **SuperBayesS** interface.

III. DARK MATTER PROTOHALOS IN THE MSSM

A. The smallest mass of the protohalo

WIMP interactions with the plasma in the early Universe produce damping of the power spectrum before and after the kinetic decoupling. Before kinetic decoupling, WIMPs behave as fluid tightly coupled to the plasma. Interactions produce shear viscosity in the WIMP fluid causing the density perturbations in the WIMP fluid to oscillate acoustically in the heat bath [13, 14]. The damping scale set by acoustic oscillations is given by the DM mass enclosed in the horizon at this epoch, i.e. the size of the horizon at kinetic decoupling [83]:

$$M_{ao} \approx \frac{4\pi}{3} \frac{\rho_\chi(T_{kd})}{H^3(T_{kd})} = 3.4 \times 10^{-6} M_\odot \left(\frac{T_{kd} g_{eff}^{1/4}}{50 \text{ MeV}} \right)^{-3}, \quad (5)$$

¹⁰ The Sommerfeld enhancement [75] is a nonrelativistic effect that depends on three quantities: the neutralino mass, the difference in mass between the neutralino and the next to the lightest particle, and the size of the coupling among them. In this context, Sommerfeld enhancement of the annihilation cross sections can significantly shift the neutralino mass consistent with the experimental $\Omega_{cdm} h^2$ value [76].

where g_{eff} is the number of effective degrees of freedom in the early Universe and ρ_χ is the DM density, both evaluated at the temperature of kinetic decoupling, T_{kd} .

After kinetic decoupling, WIMP interactions give a free-streaming scale which induces a damping of density perturbations below a scale characterized by a (comoving) free-streaming wavenumber, k_{fs} [12, 84]. Therefore, if we have perturbations contained in a sphere of radius π/k_{fs} , we have the minimal mass a DM protohalo, and then the mass of the smallest protohalo allowed by free-streaming is [83]:

$$M_{fs} \approx \frac{4\pi}{3} \rho_\chi \left(\frac{\pi}{k_{fs}} \right)^3 = 2.9 \times 10^{-6} M_\odot \left(\frac{1 + \ln(g_{eff}^{1/4} T_{kd}/50 \text{ MeV})/19.1}{(m_\chi/100 \text{ GeV})^{1/2} g_{eff}^{1/4} (T_{kd}/50 \text{ MeV})^{1/2}} \right)^3. \quad (6)$$

The mechanisms of collisional damping and free-streaming of WIMPs lead to a cutoff in the CDM power spectrum, from which the typical scale for the first haloes in the hierarchical picture of structure formation is set. The canonical value for the mass of the DM protohalos is related to the nature of the DM particle. The SUSY prediction for the size of the DM protohalos falls in a range from 10^{-11} to $10^{-3} M_\odot$ [83]. It is not clear if these first and smallest halos survive until today, since they can be destroyed either in the process of merging or by star formation. According to Refs. [24, 85], the first halos lose their mass during structure formation, but survive until today with their inner density still intact.

For a typical WIMP one finds that the chemical-decoupling temperature is given by $T_{cd} \sim m/25$, where m is the WIMP mass, and the annihilation cross section by $\langle\sigma v\rangle \sim 10^{-26} \text{ cm}^3 \text{ s}^{-1}$ in order to obtain the CDM relic density as observed today. On the other hand, the kinetic-decoupling temperature and, therefore, the minimal protohalo mass are not well constrained for WIMPs. A reference value of the minimal protohalo mass for SUSY candidates is $\sim 10^{-6} M_\odot$, which was computed by assuming a Bino-neutralino scattering with the SM particles through sfermions with a mass of around twice the neutralino mass [15, 84, 86, 87]. The chosen nature of the neutralino and the particular relation between the sfermions and Bino neutralino was well motivated by constrained SUSY extension of the SM (CMSSM), where the typically light neutralinos (lighter than 1 TeV) that are able to reproduce the correct relic density are mostly Bino that, efficiently, annihilate through sfermions in the early Universe.

Even though $M_{ph} \sim 10^{-6} M_\odot$ was a good estimate of the value of the smallest mass of the DM protohalos for a “well motivated” neutralino, it is not a strong prediction for a general neutralino DM. As described in [88], there are several ways to get a well tempered neutralino. The Bino-neutralino, that annihilates through sfermions, is one of those possibilities. Reference [83] performed a general study of the T_{cd} and T_{kd} for the MSSM neutralino, as expected $m/T_{cd} \sim 25$, while m/T_{kd} has a range of variation of almost four orders of magnitude, leading to a range in $M_{ph} \sim 10^{-12} - 10^{-3} M_\odot$. The reason of the big range of T_{kd} is that the interactions involved in the annihilation of neutralinos, that are constrained by the relic density, are not necessarily the relevant for the last scattering of neutralinos with the plasma, and therefore the relic density does not constrain it. For example, in the case of Wino-like or Higgsino-like neutralinos, the annihilation products are mainly gauge bosons, whose interactions involve different couplings with respect to the ones involved in the neutralino-fermion scattering.

It is important to mention that the computation of the kinetic decoupling temperature, and hence, the smallest protohalo mass becomes more complicated when the decoupling occurs close to the Quantum Chromodynamics (QCD) phase transition. As mentioned above, the computation of T_{kd} and M_{ph} was performed with **DarkSusy**, following the lines described in Ref. [83]. For the case of two light (u, d) and one massive s quarks, the critical temperature is assumed to be $T_c = 154 \text{ MeV}$. The plasma is described including three quarks and gluons for a temperature $T > 4T_c$. Therefore,

in the following analysis, for the regions where the kinetic decoupling temperature lies between T_c and $4T_c$ ($154 \text{ MeV} < T_{kd} < 616 \text{ MeV}$), T_{kd} will represent an upper bound while M_{ph} a lower bound.

B. The most probable regions

The determination of the smallest mass of the DM protohalo for the most probable regions of the MSSM is of great interest for the study of both direct and indirect detection of DM.

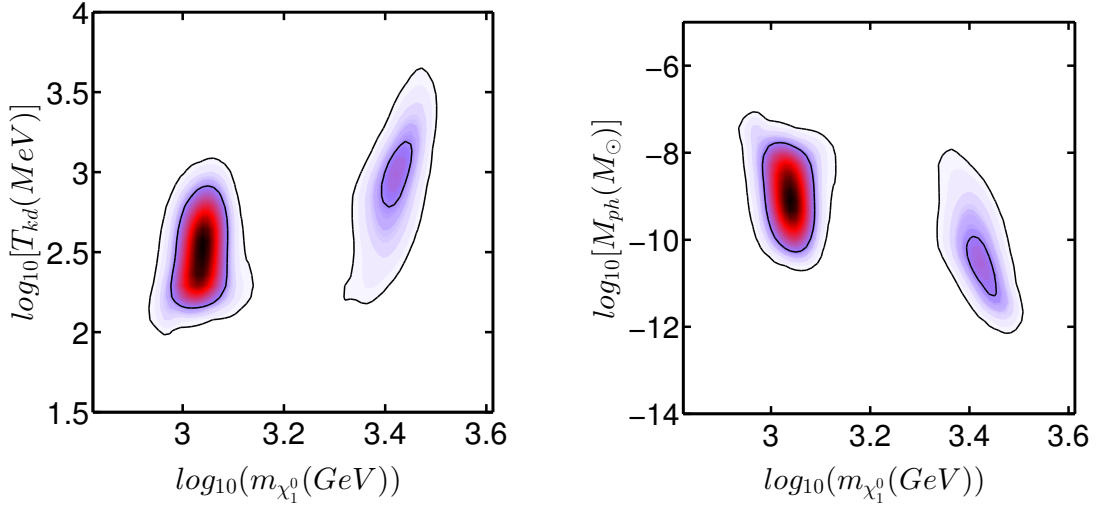


FIG. 1. The two dimensional joint posterior probability density function for the temperature of kinetic decoupling, T_{kd} , versus the neutralino mass (left panel), and for the protohalo mass, M_{ph} , versus the neutralino mass (right panel). The region with higher probability density corresponds to a Higgsino DM candidate, while in the second region the DM candidate is a Wino.

In Fig. 1 we show the two dimensional joint posterior PDF for the temperature of kinetic decoupling, T_{kd} , and for protohalo mass, M_{ph} , against the neutralino mass. The contours represent intervals at 68% and 95% credible regions. The two most probable regions are around $\sim 1 \text{ TeV}$ and $\sim 3 \text{ TeV}$ and correspond to Higgsino-like and Wino-like neutralino, respectively.

As discussed in [45], both Higgs mass measurement and relic density constraint are the main responsible for the shift of the preferred regions towards higher masses. We would like to stress that the credibility intervals represent the most probable region assuming the model that we consider is correct. In other words, the credibility regions show the relative probability density within the model. Points outside the contours are disfavored because they have worse likelihood and/or they require a large tuning to reproduce the experimental data. Concerning the prior dependence of our Bayesian analysis, we checked the stability of our results by using two different priors (I-log and S-log priors), finding that the result is basically the same; it means that our result is prior independent.

Let us describe in more details the two most probable regions. The region around 1 TeV corresponds to a Higgsino-like neutralino, whose annihilation cross section is driven by its Higgsino component (the main annihilation processes are those of a pure Higgsino-neutralino). On the other hand, for the scattering cross section, the small component of Wino and Bino plays a crucial role. The reason is the following. Assuming that sfermions are decoupled, the tree level SD scattering of Higgsino-like neutralino with fermions is mediated by the Z boson. In the limit of pure Higgsino-neutralino, \tilde{H}_u and \tilde{H}_d are degenerate, and since they have opposite quantum numbers, their contributions cancel. But then, when the gaugino masses are not decoupled, the

\tilde{H}_u and \tilde{H}_d composition of the lightest neutralino is not the same, and the cancellation does not occur. Regarding the tree level SI scattering,¹¹ the interaction is mediated by the Higgs boson, and as it interacts with the neutralinos via a Higgsino-Bino(Wino)-Higgs coupling, a nonzero gaugino component is necessary in order to have a nonzero tree level contribution. In this region sfermions are not necessarily heavy enough to be considered decoupled. However, since Higgsino-sfermion-fermion interaction is proportional to the Yukawa coupling,¹² these contributions are negligible.

The region around 3 TeV corresponds to Wino-like neutralino, where the most important annihilation interactions are those of the pure Wino neutralino. The part of the region closer to ~ 2.5 TeV has also important contributions from the neutralino-stau co-annihilation,¹³ reducing the effective annihilation rate of neutralinos in the early Universe and, therefore, decreasing the value of the neutralino mass to obtain the correct relic density, that for the case of pure Wino is ~ 3 TeV.

As in the Higgsino-like neutralino case, the tree level SD neutralino-sfermion scattering cross section receives an important contribution from the Z boson, which is the mediator of this interaction; while the tree level SI neutralino-fermion scattering cross section from a Higgs. In both cases, a non-negligible component of Bino or Higgsino is needed to have a tree-level contribution to these processes, since $\tilde{W}^0\text{--}\tilde{W}^0\text{--}Z$ and $\tilde{W}^0\text{--}\tilde{W}^0\text{--}h$ interactions do not exist. In addition, sfermions give an important contribution to the neutralino-fermions scattering cross sections, in particular for Wino-neutralinos with mass ~ 2.5 TeV. As we commented above, in this region staus are close in mass to the lightest neutralino, and selectrons and smuons are light enough to give a sizeable contribution to the scattering cross section.

C. Profile likelihood maps

In the previous section we showed that the most probable neutralino mass regions are those around 1 TeV and 3 TeV. We once again underline that this result is based on the relative probability density between the regions of the model. It does not imply that there are no valid points in the region of lighter neutralinos, i.e. in the intermediate region between 1 TeV and 3 TeV. In order to have points with good likelihood outside the 95% credibility region showed in Fig. 1, a (larger) fine-tuning which reproduces both the experimental data and the correct electroweak symmetry breaking is required.

In this subsection we study models that reproduce all the observables within 2σ confidence level. To this end, we performed a new exploration by requiring a non-negligible Bino component for the lightest neutralino. In this way we completed our previous exploration related on the study of the Higgsino-like and Wino-like neutralinos, including all the different neutralino natures. We included some of the latest ATLAS bounds on sparticle masses based on simplified models detailed in Table III. To apply the simplified model limits, we use the production cross sections published by LHC SUSY Cross Section Working Group [90], which performs an interpolation routine for gluino, squark and neutralino-chargino production. Slepton production cross section has been computed using PYTHIA 8 [91, 92]. We also include the overall signal strength of the Higgs measured by ATLAS [93]. For the computation of the branching ratios we used SUSY-HIT [94].

Figure 2 shows points that reproduce the experimental data within 2σ confidence level. We show the lightest neutralino mass as a function of the kinetic decoupling temperature, T_{kd} (top), and the protohalo mass, M_{ph} (bottom). Let us describe the mass spectrum. The characteristics

¹¹ We still assume that sfermions are decoupled.

¹² We remind that at temperatures of the order of MeV, when the kinetic decoupling occurs, the population of third generation of fermions is very small.

¹³ Sometimes solving the Boltzmann equation for the evolution of the neutralino number density to obtain the correct relic abundance of DM requires additional considerations; degeneracies in mass between the lightest neutralino and the next to the lightest one, or the presence of thresholds and resonances in the annihilation cross section may be relevant (see, e.g., the review [89]). In particular, when the lightest neutralino is close in mass to a heavier neutralino, the relic abundance is determined both by its annihilation cross section and by co-annihilation with this heavier partner that, then, decays into the lightest one. Co-annihilations may also occur with squarks, when they happen to be very close in mass to the lightest neutralino.

Topology			Luminosity	Reference
Production	Decay	Comment		
$\tilde{t}_1 \tilde{t}_1$	$\tilde{t}_1 \rightarrow b W^{(*)} \tilde{\chi}_1^0$	$m_{\tilde{t}_1} \ll m_{\chi_1^\pm}$	20.3 fb ⁻¹	[95]
$\tilde{t}_1 \tilde{t}_1$	$\tilde{t}_1 \rightarrow t \tilde{\chi}_1^0$	all hadronic	20.1 fb ⁻¹	[96]
$\tilde{b}_1 \tilde{b}_1$	$\tilde{b}_1 \rightarrow b \tilde{\chi}_1^0$		20.3 fb ⁻¹	[97]
$\tilde{g} \tilde{g}$	$\tilde{g} \rightarrow b \bar{b} \tilde{\chi}_1^0$	$m_{\tilde{q}} \gg m_{\tilde{g}}$	20.1 fb ⁻¹	[98]
$\tilde{g} \tilde{g}$	$\tilde{g} \rightarrow t \bar{t} \tilde{\chi}_1^0$	$m_{\tilde{q}} \gg m_{\tilde{g}}, 0 \text{ leptons} + 3 \text{ b-jets channel}$	20.1 fb ⁻¹	[98]
$\tilde{g} \tilde{g}$	$\tilde{g} \rightarrow q \bar{q} \tilde{\chi}_1^0$		20.3 fb ⁻¹	[28]
$\tilde{g} \tilde{g}$	$\tilde{g} \rightarrow b \bar{t} \tilde{\chi}_1^\pm$	$m_{\tilde{q}} \gg m_{\tilde{g}}, m_{\chi_1^\pm} - m_{\chi_1^0} = 2 \text{ GeV}$	20.1 fb ⁻¹	[98]
$\tilde{q} \tilde{q}$	$\tilde{q} \rightarrow q \tilde{\chi}_1^0$		20.3 fb ⁻¹	[28]
$\chi_1^\pm \chi_2^0$	$W^{(*)} \chi_1^0 Z^{(*)} \chi_1^0$	$m_{\chi_1^\pm} = m_{\chi_2^0}$	20.3 fb ⁻¹	[99]
$\tilde{l}_L^\pm \tilde{l}_L^\mp$	$\tilde{l}_L^\pm \rightarrow l^\pm \tilde{\chi}_1^0$		20.3 fb ⁻¹	[99]
$\tilde{l}_R^\pm \tilde{l}_R^\mp$	$\tilde{l}_R^\pm \rightarrow l^\pm \tilde{\chi}_1^0$		20.3 fb ⁻¹	[99]
$\tilde{l}_{LR}^\pm \tilde{l}_{LR}^\mp$	$\tilde{l}_{LR}^\pm \rightarrow l^\pm \tilde{\chi}_1^0$		20.3 fb ⁻¹	[99]

TABLE III. Simplified models exclusion limits we have included in our analysis.

of the electroweakino sector are set mainly by the fact that an efficient neutralino annihilation is needed to reproduce the correct relic density. To identify regions where the lightest neutralino co-annihilates with sfermions in the early Universe, in both left panels we highlight points that satisfy a criterion based on the mass difference between the lightest neutralino and the lightest stau (green points), and between the lightest neutralino and the lightest stops (blue points). To select those points we have required a maximal relative mass difference, $\Delta(m_{\tilde{f}} - m_{\chi_1^0})$, of 5% and a maximal absolute mass difference of 5 GeV which are imposed for neutralino masses above and below 100 GeV, respectively. The gray band of the top-right panel shows the range of temperatures where the QCD phase transition occurs, from the critical temperature to four times this one, where the value of T_{kd} represents an upper bound. Those points with a T_{kd} around the QCD phase transition are represented with lighter colors in the $m_{\chi_1^0}$ - M_{ph} plane in the bottom-left panel, where in this case the value of M_{ph} represents a lower bound.

Most of the points showed in Fig. 2 have a neutralino quasi-degenerate with another sparticle. Higgsino-like and Wino-like lightest neutralinos are quasi-degenerated with the lightest chargino, guaranteeing both a very efficient annihilation of neutralinos and co-annihilation with charginos, and selecting rather heavy neutralino masses. Neutralinos with a dominant Higgsino or Wino component cover the mass region of $m_{\chi_1^0} \gtrsim 1 \text{ TeV}$.¹⁴ As we commented in the previous section, for pure-Higgsino and pure-Wino neutralino the relic density constraint fixes the mass to $\sim 1 \text{ TeV}$ and $\sim 3 \text{ TeV}$, respectively. As a result of our scan we have identified different mixed states lying between these regions: Higgsino-Wino neutralinos, Higgsino-like and Wino-like neutralino that co-annihilate with staus or stops, and Wino-Bino neutralinos and Higgsino-like neutralino with a mass equal to half of the mass of the pseudoscalar.

Some of the points with $m_{\chi_1^0}$ slightly below 1 TeV are Higgsino-Bino neutralino. This region is strongly constrained by direct detection experiments like Xenon100 and LUX. However, there are some blind spots for μ and M_1 with opposite relative sign, as explained in detail in Refs. [34, 35].

Points with $m_{\chi_1^0} \lesssim 1 \text{ TeV}$ have a lightest Bino-like neutralino. For $100 \text{ GeV} \lesssim m_{\chi_1^0} \lesssim 600 \text{ GeV}$ it is possible to distinguish two groups of points in the bottom-left panel of Fig. 2. The first group has smaller T_{kd} , ranging from $\sim 10 \text{ MeV}$ to $\sim 100 \text{ MeV}$ and is basically aligned to the stau co-annihilation region. For these points sleptons are light, and the correct neutralino abundance was reached by slepton-neutralino co-annihilation in the early Universe. Charginos and heavier

¹⁴ Assuming DM is made of several species, the relic density constraint becomes an upper bound, allowing to have lighter Higgsino-like and Wino-like neutralinos.

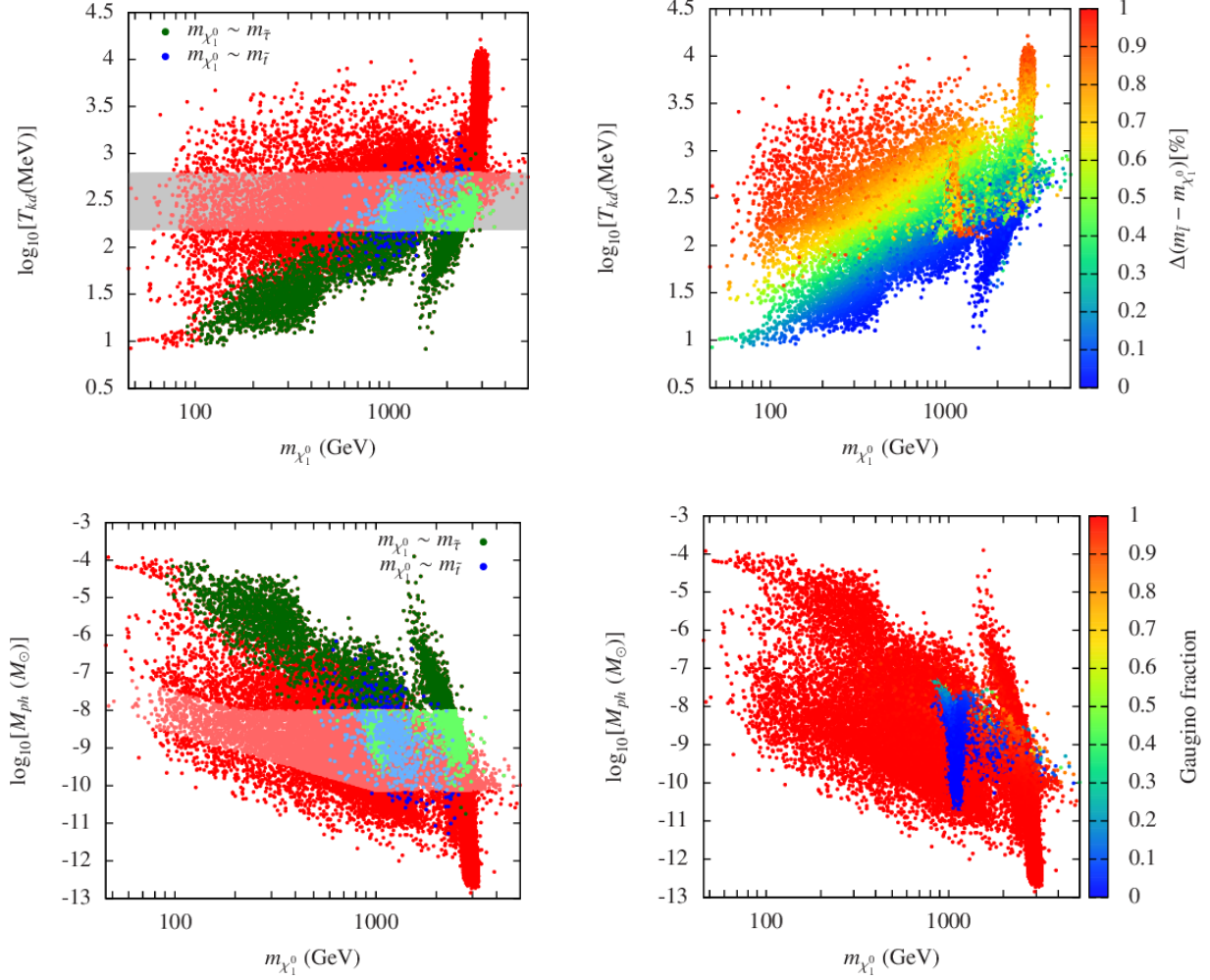


FIG. 2. Lightest neutralino mass versus T_{kd} (top panel) and M_{ph} for points that reproduce all the experimental observables within 2σ confidence level.

neutralinos are typically much heavier. For the second group of points with larger T_{kd} varying from ~ 100 MeV to ~ 3 GeV we checked that the lightest (Bino-like) neutralino is quasi degenerated with both the lightest Wino-like chargino and the second lightest neutralino, guaranteeing the neutralino annihilation. Top-right panel of Fig. 2 shows that these two regions are not completely disconnected. For example, for $\Delta(m_{\tilde{l}} - m_{\chi_1^0}) \sim 0.5$ (meaning $m_{\tilde{l}} \sim 3m_{\chi_1^0}$) sleptons also play a role in the annihilation processes.

The region $600 \text{ GeV} \lesssim m_{\chi_1^0} \lesssim 1 \text{ TeV}$ has similar characteristics, but in this case the two regions, that one with light sfermions and the other one with light chargino, have a large overlap for $30 \text{ MeV} \lesssim T_{kd} \lesssim 500 \text{ MeV}$.

Last but not least, we find that there are very few points for the Higgs and Z resonance regions. These two regions require a very large tuning, and therefore, they are very difficult to explore when requiring boundary conditions at GUT scale.

To understand the dominant process of neutralino-SM scattering in the regions we described above, in the top-right panel of Fig. 2 we show the relative mass difference between the lightest first and second generation of sleptons and the lightest neutralino, $\Delta(m_{\tilde{l}} - m_{\chi_1^0})$, while in the bottom-right panel we show the gaugino fraction.¹⁵ These plots show, for all gaugino-like neutralinos

¹⁵ The lightest neutralino is a linear combination of the superpartners of the gauge and Higgs field: $\chi_1^0 = N_{11}\tilde{B} +$

(Bino-like or Wino-like), a clear correlation between the lightest neutralino mass and the kinetic decoupling temperature for a fixed value of $\Delta(m_{\tilde{l}} - m_{\chi_1^0})$. Higgsino-like neutralinos around 1 TeV do not show a correlation for specific sleptons masses, as we comment in the previous section; its interaction with sfermions is proportional to the Yukawa coupling, and it is therefore negligible for the first and the second generation of sleptons. In the Higgsino-like case the dominant interaction is the one mediated by the Z-boson, as in the case of Bino-like and Wino-like neutralinos when sfermions are decoupled.

As we commented in section II, we assume universality and unification of squarks and slepton masses. These conditions imply that the \tilde{t}_1 and $\tilde{\tau}_1$ are the lightest squark and slepton, respectively, which is the reason why we only find neutralino-stop and neutralino-stau co-annihilation regions in our analysis. In more general scenarios where sfermions masses do not unify, the possibility of having co-annihilation with any sfermion is open, since any of them could be the next-to-LSP. If the lightest neutralino is Bino-like and the first or second generation sfermions are close enough in mass to the lightest neutralino to guarantee a large enough effective annihilation in the early universe then the dominant interaction in the scattering between the lightest neutralino and the SM particles will be the same interaction (neutralino-fermion-sfermion), producing strong correlation between the mass of the lightest neutralino and M_{ph} .

Another consequence of universality and unification is that the first and second generation of squarks are in general very heavy (due to the Higgs mass constraint to the stop sector), having, in most of the cases, a negligible contribution to the neutralino annihilation and neutralino scattering with the SM particles in the early universe. Without this assumption the most important constraint to squark masses will come from LHC bounds and direct detection experiments, allowing smaller masses. Due to the strong lower bounds on first and second generation squarks masses coming from LHC [101], one will expect that sleptons will still give the dominant contribution to the neutralino annihilation and neutralino scattering with the SM particles in the early universe for neutralinos lighter than 300 GeV. However, for neutralino masses larger than 300 GeV, contributions from first and second generation squarks could be sizeable.

Interestingly, the cases that set the smaller value of M_{ph} , when sleptons are very close in mass to the mass of the lightest neutralino, and larger value of M_{ph} , when sleptons are decoupled and the scattering is mediated by Z-boson, are covered in our analysis. On the other hand, the consequence on LHC, direct detection and indirect detection could be different, as we will discuss in the next section.

The understanding of the interactions that play a relevant role in the annihilation and scattering of neutralinos with SM particles helps us identify correlations between M_{ph} and the SUSY spectrum. These correlations could be very helpful for constraining T_{kd} indirectly from current DM experiments. In particular, the region of $m_{\chi_1^0} \lesssim 600$ GeV could be potentially tested by the LHC, as commented in Appendix A.

IV. IMPLICATIONS FOR DIRECT DETECTION

Direct detection experiments of DM look for energy deposition in the underground detector caused by scattering interactions between target nuclei and WIMPs around us. The measurement or the bound on this cross section has direct consequences on the value of the T_{kd} , assuming that the processes involved in the last scattering are the same as the ones mediated the scattering of the DM with the detectors.

$N_{12}\tilde{W}^3 + N_{13}\tilde{H}_1^0 + N_{14}\tilde{H}_2^0$. The gaugino fraction is defined by $Z_g \equiv |N_{11}|^2 + |N_{12}|^2$ (see [100] for details).

Reference [17] analyzed correlations between the mass of protohalos, M_{ph} (as well as the temperature of kinetic decoupling, T_{kd}) and the SD and SI scattering cross sections. Such a correlation appears when the mass of squarks is assumed to be large ($m_{\tilde{q}} \simeq 5\text{--}10\text{ TeV}$),¹⁶ and the dominant process for the scattering is mediated by a Z boson.

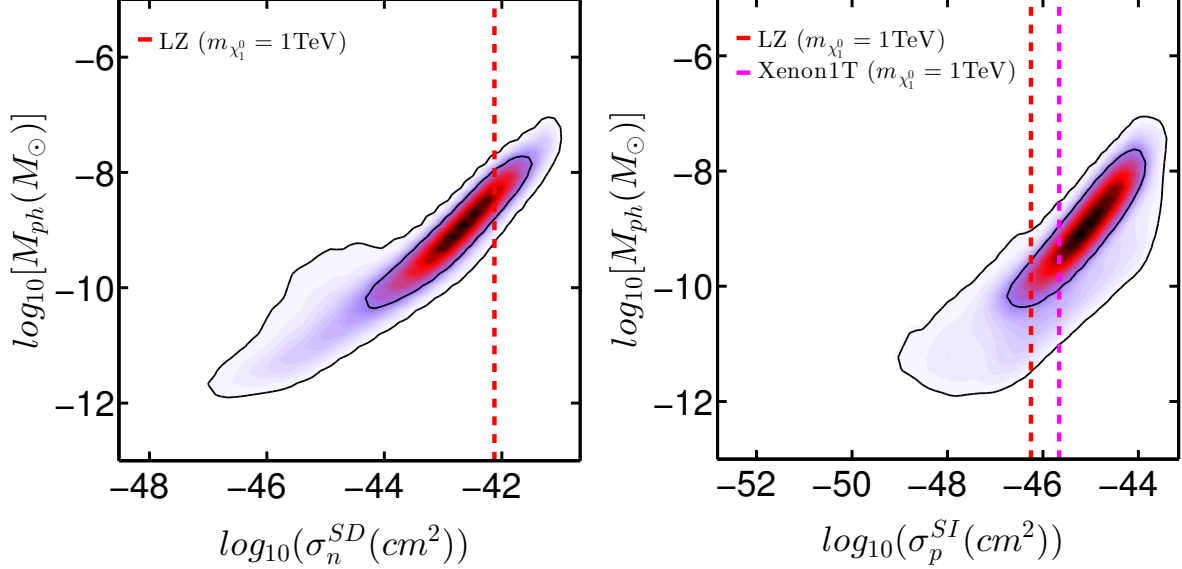


FIG. 3. Most probable regions on the scattering cross section–protohalo mass plane. The left and right panels show the correlation with the spin-dependent and spin-independent cross sections, σ_n^{SD} and σ_p^{SI} , respectively.

In Fig. 3, we show the most probable region on the plane of the protohalo mass, M_{ph} , and the SD and the SI cross sections computed at tree level. Contrary to Fig. 1, the probability regions do not have disconnected parts, but they include both Higgsino-like (at $\sim 1\text{ TeV}$) and Wino-like (at $\sim 3\text{ TeV}$) neutralinos. In both cases the dominant scattering process is mediated by the Z-boson. We see how the expected improvement on the SI sensitivity by, e.g., Xenon1T [102] and LUX-Zeppelin experiment (LZ) [103], will reduce the most probable range of the minimal subhalo mass down to below $\sim 10^{-9} M_\odot$, while the expected SD sensitivity provides weaker constraints.

Since in the analysis we have included the XENON100 limits as constraints on the WIMP-nucleon scattering cross section, we see in the right panel of Fig. 3 that the region around $\sigma_p^{SI} \approx 2 \times 10^{-44} \text{ cm}^2$ is strongly penalized. The current LUX bound is more stringent on the spin-independent sensitivity, giving an upper bound of $\sigma_p^{SI} \approx 10^{-44}$ for a 1 TeV neutralino [104], although we did not include it in our analysis. Including the LUX bound, therefore, would affect the very right part of the right panel of Fig. 3 (and also Fig. 5 shown below). However, since the regions affected are tiny, it would not affect our conclusions.

Figure 4 shows points that reproduce the experimental constraint at 2σ confidence level for the minimal protohalo mass versus the tree level SD cross section plane. The right panel shows the case where the lightest first or second generation of sfermions is at least nine times heavier than the lightest neutralino, $\Delta(m_{\tilde{l}_{\tilde{q}}} - m_{\chi_1^0}) > 0.8$. The thin yellow line corresponds to $\sim 1\text{ TeV}$ Higgsino-like neutralino, while the thin red line to $\sim 3\text{ TeV}$ Wino-like neutralino. In these two cases the Z-boson mediates both scattering processes. The rest of the points correspond to the Bino-like neutralino where, instead of a line, we get scattered points with $100\text{ GeV} \lesssim m_{\chi_1^0} \lesssim 1\text{ TeV}$. We remind that for

¹⁶ The authors of Ref. [17] used the squark mass to show the effect of light sfermions in the correlation, but clarify that when the correlation is broken, the relative contribution from squark, especially the slepton exchange in the kinetic decoupling process, increases.

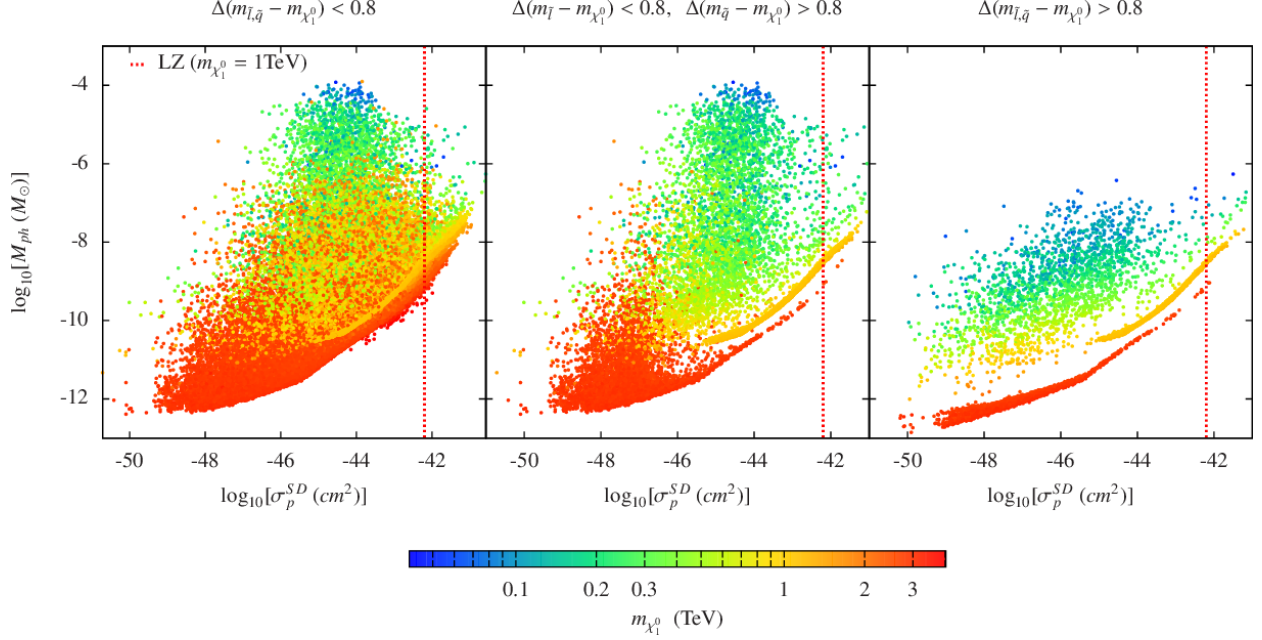


FIG. 4. Points that reproduce all the experimental observables at 2σ confidence level in the SD cross section σ_p^{SD} versus protohalo mass M_{ph} plane. The neutralino mass is indicated with colors, as shown in the color bar. The three panels separate the points in three groups: light squarks and sleptons (left panel), light sleptons and decoupled squarks (central panel), and decoupled squarks and sleptons (right panel).

the Bino-like case the annihilation cross section and, therefore, the relic density can be adjusted varying the neutralino mass and its mass splitting with the lightest (Wino-like) chargino. On the other hand, even if it is ten times heavier than the lightest neutralino, sleptons mediate the dominant scattering processes that set T_{kd} for most of the points. The size of the contribution of processes, mediated by the Z-boson, depends on how large the Higgsino component of the neutralino is. However, the Higgsino component of a Bino-like neutralino is highly constrained by SI cross sections bounds. Nevertheless, as we comment in subsection III C, there are some blind spots for SI cross sections. For those points the Z-boson gives an important contribution to the scattering cross section.

Regarding σ_p^{SD} for the Bino-like region, the dominant process is mediated by the Z-boson.¹⁷ Besides the dominant scattering processes for T_{kd} and σ_p^{SD} are different, there is an apparent correlation between the two quantities for a fixed neutralino mass. We have checked the behavior of the correlation for a specific values of $m_{\chi_1^0}$, finding that T_{kd} spreads around one order for a given value of σ_p^{SD} .

Another characteristic of the Bino-like case, assuming sfermions are heavy, is that the minimal protohalo mass is the one allowed by the free-streaming. On the contrary, for the Higgsino-like and Wino-like cases, the minimal protohalo mass is the one allowed by the damping scale set by acoustic oscillation.

Central panel of Fig. 4 shows the case where the lightest slepton has a mass smaller than ~ 10 times the lightest neutralino mass. As expected, the Wino-like and Bino-like regions spread to larger protohalo masses.¹⁸ Left panel of Fig. 4 shows the case where the lightest sleptons and

¹⁷ Squarks are typically heavier than sleptons when parameterizing the model at gauge coupling unification scale. Therefore, imposing the condition $\Delta(m_{\tilde{l}} - m_{\chi_1^0}) > 0.8$ implies that squarks are typically much heavier than ten times the mass of the lightest neutralino.

¹⁸ Winos and Binors have strong SD interaction since diagrams where the incoming and outgoing fermions have the same helicity are allowed. On the other hand, the diagrams where the incoming and outgoing fermions have opposite helicities are spin-independent, requiring a $q\tilde{q}\tilde{H}$ vertex to yield the helicity flip, which is Yukawa suppressed. For a review, see Ref [105].

squarks are smaller than ~ 10 times the lightest neutralino. Here, squarks are light enough to give important contributions to the scattering with the nucleus, spreading the points to larger values of σ_n^{SD} .

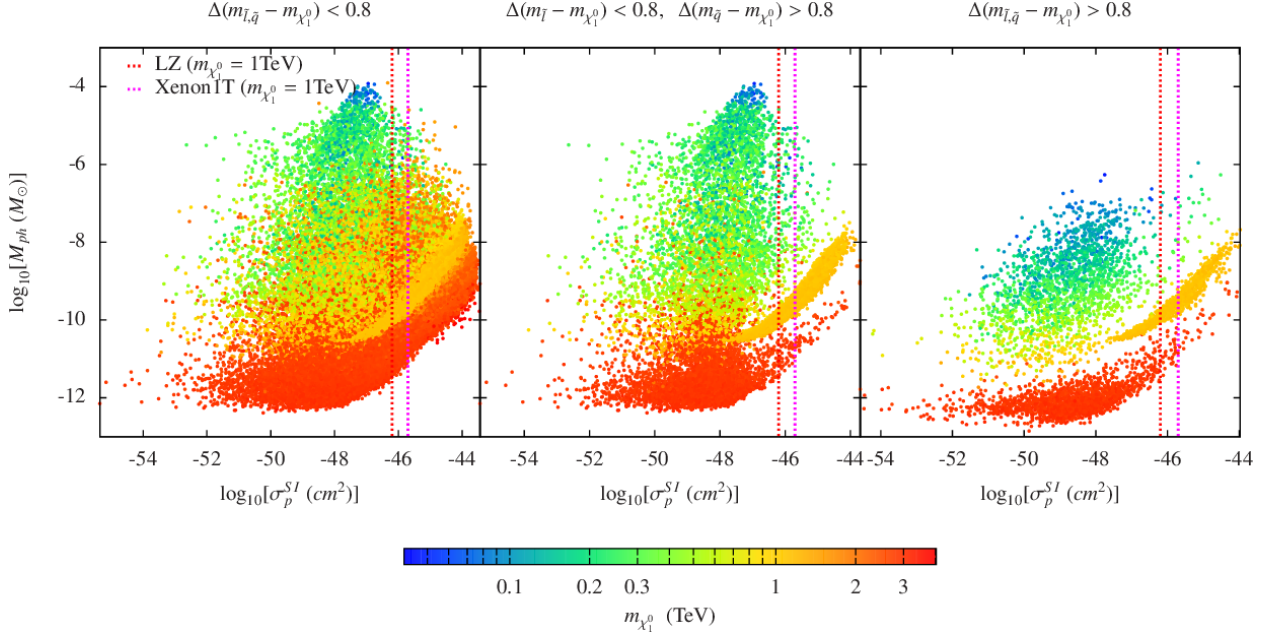


FIG. 5. Same as Fig. 4 for the the SI cross section, σ^{SI} .

Figure 5 shows points in the minimal protohalo mass versus tree level SI cross section plane. The main contribution to the SI cross section comes from the Higgs exchange, requiring a non-negligible Higgsino and Wino/Bino coupling (since Higgs couplings through neutralinos are $H\tilde{H}\tilde{B}$ and $H\tilde{H}\tilde{W}$). On the other hand, the total neutralino-SM scattering, and therefore T_{kd} and M_{ph} , are dominated by SD interactions. As a consequence, right panel of Fig. 5 shows the correlation between the $Z\chi_1^0\chi_1^0$ and $H\chi_1^0\chi_1^0$, for the Higgsino and Wino case. Central and left panels show the effect of sleptons and squarks in the scattering processes.

Figures 4 and 5 show the expected sensitivity by Xenon1T and LZ assuming the neutralino mass is ~ 1 TeV. For a neutralino of ~ 100 GeV, the expected sensitivity is around one order of magnitude stronger.

As we commented in the previous section, assuming universality and unification of the squark masses and slepton masses, we impose a particular mass hierarchy: \tilde{t}_1 is the lightest squark and $\tilde{\tau}_1$ is the lightest slepton. Without this assumption, first and second generation of sfermions can be lighter and change the phenomenology for direct detection experiments and colliders. In the case that the lightest neutralino is gaugino-like and the first and second generation of squarks are the lighter sfermions, T_{kd} will be completely correlated with the neutralino-nucleon scattering cross section. Still, if they are not the lightest ones but they are significantly lighter than in our analysis the neutralino-nucleon scattering cross section could increase, getting values close to the actual limits. In addition, if they are lighter or close in mass to the first and second generation sleptons, the scattering of the neutralino with SM particles in the early universe could also increase. Those points will most likely populate the top-right corner of the left panel of Figs. 4 and 5.

Notice that, as we mentioned above, for the computation of SI cross sections we have adopted $f_{Ts} = 0.36$ for the contribution of the strange quark to the nucleon form factors [72], derived experimentally from measurements of the pion-nucleon sigma term. However this value is considerably larger than determinations obtained from lattice QCD, $f_{Ts} = 0.043 \pm 0.011$ [106]. The

discrepancy between the two values and its impact in the SI cross section is studied in more detail in Refs. [107, 108].

Finally, we remind that the scattering cross-sections considered in this work were computed at tree level. In the cases where neutralino approaches to a pure state (Bino, Wino or Higgsino), this approximation may not give a reliable result. In particular, in the case of the Wino-neutralino, one loop corrections give the dominant contributions (see, e.g. Ref. [109, 110]).

V. IMPLICATIONS FOR INDIRECT DETECTION

One of the most reliable methods to model the non-linear evolution of DM is numerical simulation, although it is limited by mass resolution. In fact, the minimum self-bound mass (M_{min}) of DM halos is expected to be many orders of magnitude below the resolution of current simulations. Through numerical simulations such as *Acquarius* [111], we can obtain information on the subhalo hierarchy, although its resolution mass limit $\sim 10^4$ or $\sim 10^5 M_\odot$ is far from the predicted protohalo mass shown in Sec. III.

Here we investigate the impact of different values of M_{min} on the gamma-ray luminosity due to DM annihilation, and compute a boost factor of a given halo of mass M due to the substructure inside it, by integrating the subhalo annihilation luminosities from the protohalo mass we have found, M_{ph} , up to the mass of sizable fraction of the host halo M_{max} . The total luminosity of the DM halo due to annihilation is proportional to:

$$L \propto \int_{M_{ph}}^{M_{max}} dM \frac{dn}{dM} L_{sh}(M), \quad (7)$$

where dn/dM is the subhalo mass function, i.e. the subhalo number density per unit mass range. Numerical simulations find that the differential subhalo mass function follows a power law $dn/dM \propto M^{-\beta}$, with $\beta \sim 1.9$ or $\beta \sim 2$ (see, e.g. [112, 113]). We adopt a M^{-2} subhalo mass spectrum as our fiducial subhalo model.

We assume that each individual DM subhalo is described by a Navarro-Frenk-White (NFW) density profile [114]:

$$\rho_{sh} = \frac{\rho_s}{(r/r_s)(1 + r/r_s)^2}, \quad (8)$$

where ρ_s and r_s are the characteristic density and radius, respectively. $L_{sh}(M)$ is defined as the luminosity of each subhalo in the host halo, which depends on the volume integral of the subhalo density squared, and is given by:

$$L_{sh}(M) = \int dV_{sh} \rho_{sh}^2 \propto \rho_s^2 r_s^3. \quad (9)$$

Following the same approach of Ref. [115], we parameterize the scaling relation between the gamma-ray luminosity and subhalo mass as:

$$L_{sh}(M) \propto L_0 \times \begin{cases} \left(\frac{M}{10^4 M_\odot}\right)^{0.77}, & M > 10^4 M_\odot \\ \left(\frac{M}{10^4 M_\odot}\right)^\gamma, & M < 10^4 M_\odot, \end{cases} \quad (10)$$

where above the simulation resolution of $\sim 10^4 M_\odot$, the luminosity versus subhalos mass scales as $L \propto M^{0.77}$, while below the resolution we assume $\gamma < 1$. Here L_0 encodes all the particle

physics, i.e., $L_0 \propto \langle \sigma v \rangle / m_{\chi_1^0}^2$, where $\langle \sigma v \rangle$ is the velocity-averaged annihilation cross section times the relative velocity.¹⁹

In order to obtain the scaling behavior of $L_{\text{sh}} \propto M^{0.77}$, we adopted scaling relations among several quantities found in the *Aquarius* numerical simulation. Since each subhalo is described by a NFW density profile, we related the maximum rotation velocity of the subhalo, V_{max} , and the radius at which the rotation curve reaches this maximum, r_{max} , with the characteristic density and radius, ρ_s and r_s , to obtain them as a function of the subhalo mass M . These empirical relations between $(V_{\text{max}}, r_{\text{max}})$ and (ρ_s, r_s) , however, lose validity in mass regions below the resolution limit of the simulation. For this reason we split Eq. (10) in two terms, above and below the resolution ($10^4 M_\odot$), where in the latter we put γ as a phenomenological parameter describing the scaling behavior.

The luminosity in Eq. (7) can be then written as:

$$L \propto \frac{\langle \sigma v \rangle}{m_{\chi_1^0}^2} \left[\int_{M_{\text{ph}}}^{10^4 M_\odot} dM M^{-2} \left(\frac{M}{10^4 M_\odot} \right)^\gamma + \int_{10^4 M_\odot}^{M_{\text{max}}} dM M^{-2} \left(\frac{M}{10^4 M_\odot} \right)^{0.77} \right]. \quad (11)$$

Assuming that the first term dominates, the luminosity is, thus, a function of the protohalo mass:

$$L(M_{\text{ph}}) \sim \frac{\langle \sigma v \rangle}{m_{\chi_1^0}^2} \left(\frac{M_{\text{ph}}}{10^4 M_\odot} \right)^{\gamma-1}. \quad (12)$$

For comparison, we define a reference value for such a luminosity, L_{ref} , as:

$$L_{\text{ref}} \propto \frac{\langle \sigma v \rangle_{\text{ref}}}{m_{\chi_1^0}^2} \left(\frac{M_{\text{ref}}}{10^4 M_\odot} \right)^{\gamma-1}. \quad (13)$$

For values of these reference parameters, we adopt $\langle \sigma v \rangle_{\text{ref}} = 3 \times 10^{-26} \text{ cm}^3 \text{ s}^{-1}$, $M_{\text{ref}} = 10^{-6} M_\odot$, and $\gamma = 0.8$.

The left panel of Fig. 6 shows the two-dimensional joint posterior PDF for the protohalo mass M_{ph} and $\langle \sigma v \rangle$ with 68% and 95% credible contours. These most probable regions fall in a mass range between 10^{-7} and $10^{-12} M_\odot$, and $\langle \sigma v \rangle = 10^{-26} - 10^{-24} \text{ cm}^3 \text{ s}^{-1}$. The region with higher probability density again corresponds to a Higgsino DM candidate with the annihilation cross section close to the canonical value $10^{-26} \text{ cm}^3 \text{ s}^{-1}$, while the second region corresponds to a DM Wino candidate with much larger annihilation cross section $\sim 10^{-24} \text{ cm}^3 \text{ s}^{-1}$. In the right panel we show the ratio of the luminosity over the reference one $\tilde{L} \equiv L/L_{\text{ref}}$, versus the DM mass, $m_{\chi_1^0}$. We also analyzed the change in the boost by varying the γ -parameter in a range between 0.5 and 0.9, we only show the case $\gamma = 0.8$, and found that \tilde{L} always got largely boosted by decreasing γ . This behavior depends on the normalization made on the protohalo mass, M_{ph} , since it has been normalized to the limit of the numerical simulation ($10^4 M_\odot$).

Figure 7 shows the boost factor, $\tilde{L} \equiv L/L_{\text{ref}}$, for points that reproduce all the experimental observables within 2σ confidence level. Right panel shows points which refer to a Higgsino-like and Wino-like neutralinos, while the left panel shows points where the neutralino is mostly Bino-like. Bino-like neutralinos have very small $\langle \sigma v \rangle$ in the limit of zero velocity. Co-annihilations, which play a very important role in the efficient annihilation in the early Universe, are not present anymore; this is the reason for which we have a very small boost of the luminosity.

Finally we comment that although not included in this work, Fermi and HESS bounds on $m_{\chi_1^0} - \langle \sigma v \rangle$ plane strongly constrain the wino-like region, excluding the region around 2.4 TeV; see Refs. [116–119].

¹⁹ In the considered MSSM, for almost all the data points, we find that the annihilation cross section, $\langle \sigma v \rangle$, is almost independent of velocity, $\langle \sigma v \rangle \approx (\sigma v)_0$.

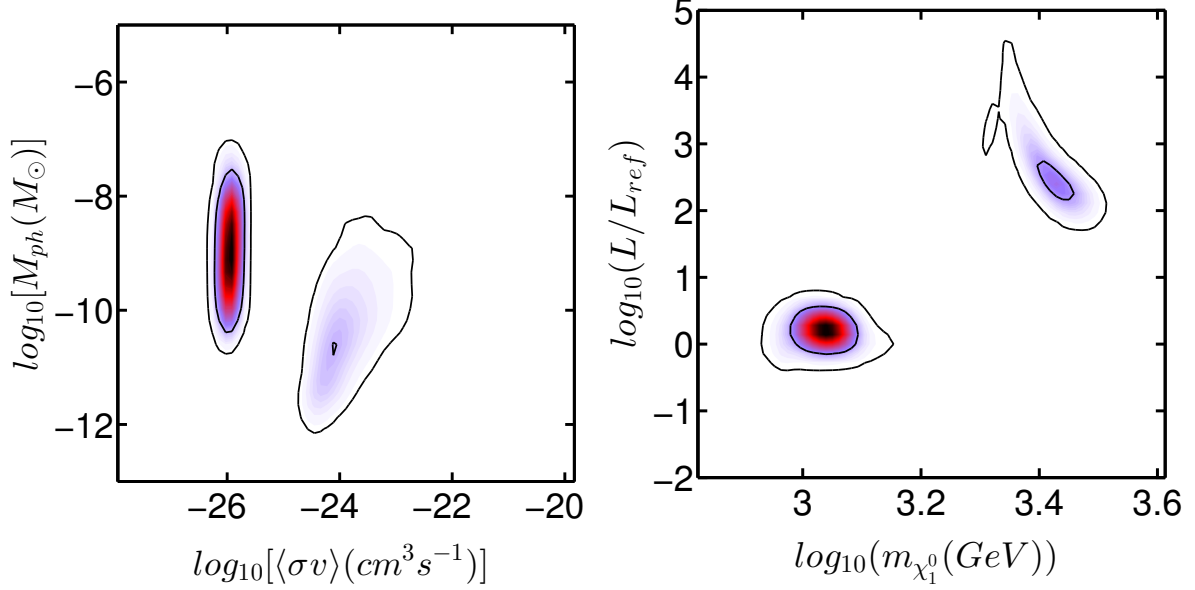


FIG. 6. The two dimensional joint posterior probability density function for the protohalo mass, M_{ph} , versus the velocity-averaged annihilation cross section times the relative velocity, $\langle\sigma v\rangle$ (left panel), and for \tilde{L} , obtained by using $\gamma = 0.8$, versus the Dark Matter particle mass, $m_{\chi_1^0}$ (right panel). For both panels, the region with higher probability density corresponds to a Higgsino DM candidate; in the second region the DM candidate is a Wino. Left panel shows that, in the Higgsino case, the protohalo mass M_{ph} is lower than the reference one, while $\langle\sigma v\rangle$ does not deviate from $\langle\sigma v\rangle_{ref} \sim 10^{-26} \text{ cm}^3 \text{ s}^{-1}$. Right panel shows that, in the Wino case, the protohalo mass M_{ph} is even lighter and $\langle\sigma v\rangle$ is two orders of magnitude larger than $\langle\sigma v\rangle_{ref} \sim 10^{-26} \text{ cm}^3 \text{ s}^{-1}$; thus, there is a substantial enhancement of \tilde{L} .

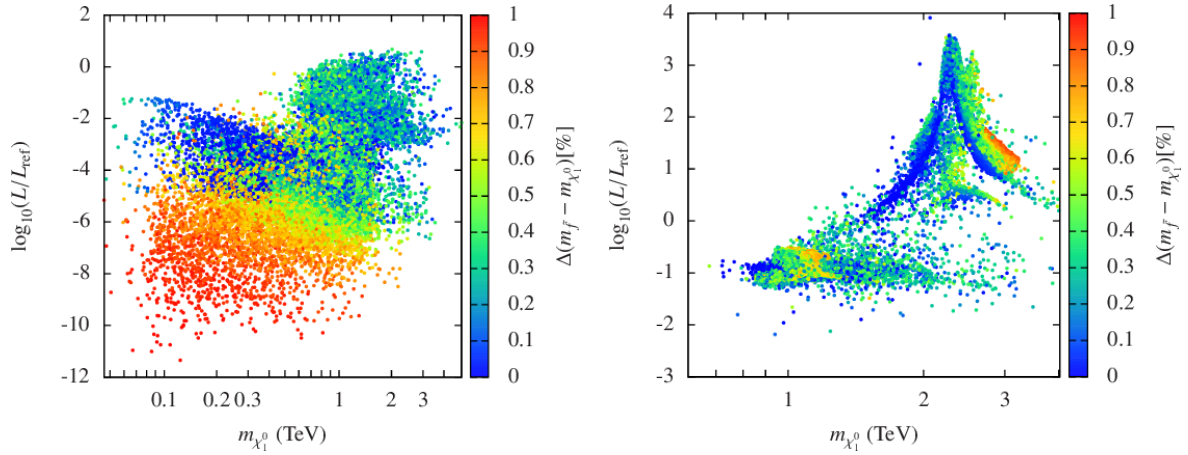


FIG. 7. The mass of the lightest neutralino versus the boost factor, $\tilde{L} \equiv L/L_{ref}$, for points that reproduce all the experimental observables within 2σ confidence level. Left panel shows points which refer to a Bino-fraction (N_{11}) larger than 0.8. Right panel shows point with a Bino-fraction smaller than 0.8

VI. SUMMARY AND CONCLUSIONS

In this work we have studied how the kinetic decoupling of dark matter could improve our knowledge of the properties of the dark matter protohalos within a supersymmetric model, i.e. the Minimal Supersymmetric extension of the Standard Model. Such a model is the well-motivated extension of the Standard Model at the electroweak scale. At first, it was introduced to solve

the hierarchy problem of the Standard Model, but it revealed to have many other interesting characteristics. In particular, it contains a tempting particle dark matter candidate, the lightest neutralino. If such a neutralino is the lightest supersymmetric particle and the quantum number R-parity is preserved, it is stable, yielding to a thermal abundance as that indicated by the observed dark matter density.

In our analysis we do a forecast on the mass of the protohalos within a supersymmetric framework realized with 9 independent parameters. We performed any analysis in the light of the latest data coming from particle physics experiments, as well as the relic density constraints. Among them, the most important observables involved in the analysis, which give a relevant impact on our results, are the mass of the Higgs and the relic density.

1. The kinetic-decoupling temperature and, thus, the minimal protohalo mass result to be not well constrained for WIMPs, since the interactions involved in the annihilation of neutralinos, that are constrained by the relic density, are not necessarily those which participate in the scattering of neutralinos with first and second generation of fermions. In a supersymmetric framework, the minimal protohalo mass is typically $10^{-6}M_{\odot}$, assuming a Bino-neutralino annihilating through sfermions with a mass of around twice the neutralino mass. This resulted in a possible option to get a well tempered neutralino. In addition, this possibility has been well motivated by constrained scenarios like CMSSM, affirming that when the neutralino is mostly Bino, it efficiently annihilates through sfermions in the early Universe, giving the correct relic density. Nevertheless, it was in tension with the experimental data within the CMSSM, especially after the first run of the LHC, where a considerable part of this region was excluded.
2. Using a Bayesian framework, we showed that the most probable neutralino mass regions satisfying both the Higgs mass and the relic density constraints, are those with the lightest supersymmetric neutralino mass around 1 TeV and 3 TeV, that correspond to Higgsino-like and Wino-like neutralino, respectively. We mentioned that, concerning the Higgsino-like neutralino, the annihilation cross section is driven by its Higgsino component, while for Wino-like neutralino, the annihilation cross section is mainly driven by its Wino component. We also discussed that the part of the region closer to ~ 2.4 TeV gets important contributions from the neutralino-stau co-annihilation, reducing both the effective annihilation rate of neutralinos in the early Universe and the value of the neutralino mass, in order to obtain the correct relic density.
3. We commented that in the case of Wino-like or Higgsino-like neutralinos the annihilation products are gauge bosons, whose interactions involve different couplings with respect to the ones of the neutralino-fermion scattering. For that reason kinetic decoupling temperature, T_{kd} , exhibits a considerable range of variation, that reflects, in turn, to a protohalo mass range of $M_{ph} \sim 10^{-12}-10^{-7}M_{\odot}$.
4. We also discussed the Bino like neutralino with masses smaller than ~ 1 TeV, where a quasi-degenerated sfermion or chargino, or a light sfermion are necessary to get the correct dark matter abundance. Sleptons give the most important contribution for the kinetic decoupling temperature and therefore to the protohalo mass, setting the range $M_{ph} \sim 10^{-11}-10^{-4}M_{\odot}$.
5. Kinetic decoupling of dark matter, involving elastic scattering of a dark matter particle with Standard Model particles in the early Universe, reveals a relevant process for dark matter direct detection searches. In our analysis, we showed that the regions where the probability is higher the correlation between the protohalo mass and experimental signatures permits to put constraints on the protohalo mass. We depicted how improvements

on the spin-independent sensitivity might reduce the most probable range of the protohalo mass between $\sim 10^{-9} M_\odot$ and $\sim 10^{-7} M_\odot$, while constraints associated to the expected spin-dependent sensitivity are weaker. To give this conclusion we computed scattering cross sections at tree-level. However, specially in the Wino-like neutralino case, loop corrections should be considered since the tree level coupling vanishes when approaching the pure Wino case.

6. We discussed, as well, how the interplay among both spin-dependent and spin-independent scattering processes, strongly depends on the neutralino composition. For both Higgsino-like and Wino-like cases, the spin-dependent scattering between Higgsino and fermions is mediated dominantly by the Z boson at tree level, while for the spin-independent scattering, the interaction is mediated by the Higgs boson. Regarding the Higgsino neutralino, we commented that the spin-independent interaction gives a nonzero tree-level contribution as long as gauginos are not decoupled, a non-negligible Bino or Wino component is necessary to have a non-negligible coupling with the Higgs. On the other hand, for the Wino-like neutralino the requirement of a non-negligible component of Higgsino is indispensable to have a tree-level contribution to both scattering processes if sfermions are decoupled.
7. Depending on the nature of neutralino, the value of the annihilation cross section, $\langle\sigma v\rangle_{v\rightarrow 0}$, changes by different orders of magnitude. We presented that the annihilation cross section, $\langle\sigma v\rangle$, in the Higgsino case does not deviate from the canonical cross section, $\langle\sigma v\rangle \sim 10^{-26} \text{ cm}^3 \text{ s}^{-1}$. On the other hand, in the Wino case non-perturbative effect is important, $\langle\sigma v\rangle$ increases up to two orders of magnitude. And it is much smaller in the Bino-like case, where co-annihilations with sfermions played a crucial role to fix the correct abundance.
8. Another way to look for dark matter is through indirect detection methods, which consist to detect, *indirectly*, the lightest supersymmetric particle through annihilation processes where Standard Model particles, including gamma-ray photons, are produced. Since the luminosity of each subhalo in the host halo due to the dark matter annihilation processes depends on the volume integral of the subhalo density squared, smaller and denser substructures provide an enhancement of the luminosity. In this work, we showed for both neutralino Higgsino-like and Wino-like cases how the boost of the luminosity due to dark matter annihilation increases, depending on the protohalo mass. We discussed that in the Higgsino case, there is no a significant enhancement of the luminosity: the protohalo mass is lower than the standard value often used in the literature of $\sim 10^{-6} M_\odot$, while $\langle\sigma v\rangle$ does not deviate from $\langle\sigma v\rangle \sim 10^{-26} \text{ cm}^3 \text{ s}^{-1}$. In the Wino case, a substantial enhancement of the luminosity is seen: the protohalo mass reaches lighter values, and $\langle\sigma v\rangle$ is two orders of magnitude larger.

ACKNOWLEDGMENTS

The work was supported partly by NWO through Vidi grant (S.A.), by University of Amsterdam (R.D. and S.A.) and by Fundação de Amparo à Pesquisa do Estado de São Paulo (M.E.C.C.). R.D. kindly acknowledges Francesca Calore and Sergio Palomares Ruiz for interesting and stimulating discussions. R.D. also thanks Miguel Nebot and Sebastian Liem for useful comments. M.E.C.C. thanks Andre Lessa and Boris Panes for useful discussions.

Appendix A: Implications for collider searches

As commented in Sec. III C, points with $m_{\chi_1^0}$ smaller than ~ 1 TeV are Bino-like and require a light enough next-to-lightest sparticle, in order to guarantee an efficient annihilation in the early Universe. Based on the characteristics of the next-to-lightest sparticle, we are going to comment the potential LHC signatures.

For neutralinos lighter than 500 GeV there are two regions, in addition to Z/h/A resonances. The first one has χ_1^\pm close in mass to χ_1^0 . A light Wino-like chargino which annihilates and co-annihilates in the early Universe is required, and is represented by points with $5 \text{ GeV} \lesssim m_{\chi_2^0} - m_{\chi_1^0} \lesssim 40 \text{ GeV}$ in the left panel of Fig. 8. In this region χ_1^0 is dominantly Bino and χ_1^\pm and χ_2^0 are dominantly Winos. The Bino and Wino mass, M_1 and M_2 , are close to the values where the tree level decay of χ_2^0 to $Z^{(*)}\chi_1^0$ is suppressed, and the branching ratio to $\gamma\chi_1^0$ acquires a large value, as discussed in detail in Refs. [120, 121]. Right panel of Fig. 8 shows that some of the points can have a dominant $\chi_2^0 \rightarrow \gamma\chi_1^0$ decay, giving a characteristic signature at collider. Moreover, the decay channel $\tilde{l}_L \rightarrow l\chi_2^0 \rightarrow l\gamma\chi_1^0$ becomes relevant. Although the photon produced in the χ_2^0 and \tilde{l}_L decays is very soft, it could give a clear signature at collider in the boosted regime. Keep in mind that a potential measurement of sleptons will directly constraint the prediction for the protohalo mass for Bino-like neutralino.

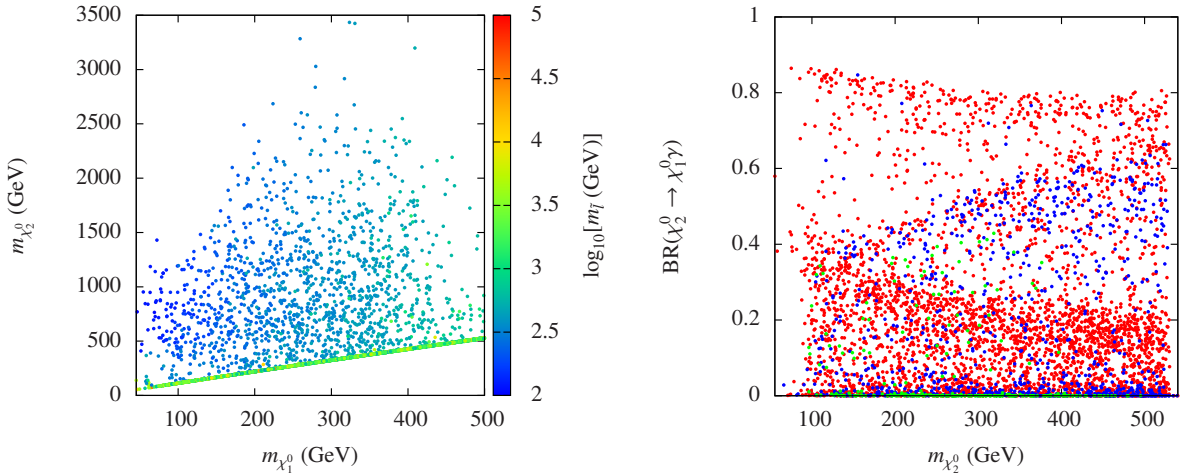


FIG. 8. Left panel shows the χ_1^0 mass and χ_2^0 mass plane. The colors show the mass of the lightest slepton ($\tilde{e}_{L,R}, \tilde{\mu}_{L,R}$). Right panel shows the branching ratio of χ_2^0 to photons as a function of χ_2^0 mass for points with $m_{\tilde{l}_L} > m_{\chi_2^0}$. Red, blue and green points correspond to $m_{\tilde{l}_L} > 1 \text{ TeV}$, $500 \text{ GeV} < m_{\tilde{l}_L} < 1 \text{ TeV}$ and $m_{\tilde{l}_L} < 500 \text{ GeV}$ respectively.

The second region corresponds to stau co-annihilation, where $\tilde{\tau}_1$ and χ_1^0 are very close in mass. In the left panel of Fig. 8 the points outside $5 \text{ GeV} \lesssim m_{\chi_2^0} - m_{\chi_1^0} \lesssim 40 \text{ GeV}$ correspond to this region. Notice that, as a consequence of universality conditions of slepton soft masses, the first and second generation of sleptons is relatively close in mass to the lightest stau and, therefore, to the lightest neutralino. The authors of Ref. [122] discuss the status of this region after the first run of the LHC in the framework of the constrained MSSM (CMSSM), and project the likely sensitivity of the LHC searches in Run 2 at 14 TeV center of mass energy and 300/fb of integrated luminosity, concluding that the entirely CMSSM co-annihilation strip will be tested.

For $m_{\chi_1^0} \gtrsim 500 \text{ GeV}$ new regions arise. Stop co-annihilations, and neutralino annihilations are mediated by sfermions. In this neutralino mass range the production of colored particles is the most promising. In Refs. [123–125], is studied the stop co-annihilation region, not only by direct stop production but also by gluino production, where direct stop productions constraint light stops

($m_{\tilde{t}_1} \lesssim 400$ GeV); for heavier stops gluino, the production seems to be more promising. On the other hand, the region where neutralino annihilation is mediated by squarks is directly constrained by limits on squarks masses.

-
- [1] G. Jungman, M. Kamionkowski, and K. Griest, Phys.Rept. **267**, 195 (1996), arXiv:hep-ph/9506380 [hep-ph].
 - [2] L. Bergstrom, Rept.Prog.Phys. **63**, 793 (2000), arXiv:hep-ph/0002126 [hep-ph].
 - [3] G. Bertone, D. Hooper, and J. Silk, Phys.Rept. **405**, 279 (2005), arXiv:hep-ph/0404175 [hep-ph].
 - [4] C. Munoz, Int.J.Mod.Phys. **A19**, 3093 (2004), arXiv:hep-ph/0309346 [hep-ph].
 - [5] J. L. Feng, Ann.Rev.Astron.Astrophys. **48**, 495 (2010), arXiv:1003.0904 [astro-ph.CO].
 - [6] 1343079, (2015), arXiv:1502.01589 [astro-ph.CO].
 - [7] D. Hooper and S. Profumo, Phys.Rept. **453**, 29 (2007), arXiv:hep-ph/0701197 [hep-ph].
 - [8] S. P. Martin, (1997), arXiv:hep-ph/9709356.
 - [9] K. A. Meissner and H. Nicolai, Phys.Lett. **B648**, 312 (2007), arXiv:hep-th/0612165 [hep-th].
 - [10] M. Gogberashvili, Int.J.Mod.Phys. **D11**, 1635 (2002), arXiv:hep-ph/9812296 [hep-ph].
 - [11] J. A. Casas, J. M. Moreno, S. Robles, K. Rolbiecki, and B. Zaldivar, (2014), arXiv:1407.6966 [hep-ph].
 - [12] A. M. Green, S. Hofmann, and D. J. Schwarz, JCAP **0508**, 003 (2005), arXiv:astro-ph/0503387 [astro-ph].
 - [13] A. Loeb and M. Zaldarriaga, Phys.Rev. **D71**, 103520 (2005), arXiv:astro-ph/0504112 [astro-ph].
 - [14] E. Bertschinger, Phys.Rev. **D74**, 063509 (2006), arXiv:astro-ph/0607319 [astro-ph].
 - [15] S. Hofmann, D. J. Schwarz, and H. Stoecker, Phys.Rev. **D64**, 083507 (2001), arXiv:astro-ph/0104173 [astro-ph].
 - [16] S. Profumo, K. Sigurdson, and M. Kamionkowski, Phys.Rev.Lett. **97**, 031301 (2006), arXiv:astro-ph/0603373 [astro-ph].
 - [17] J. M. Cornell and S. Profumo, JCAP **1206**, 011 (2012), arXiv:1203.1100 [hep-ph].
 - [18] M. Cabrera, J. Casas, and A. Delgado, Phys.Rev.Lett. **108**, 021802 (2012), arXiv:1108.3867 [hep-ph].
 - [19] G. F. Giudice and A. Strumia, Nucl.Phys. **B858**, 63 (2012), arXiv:1108.6077 [hep-ph].
 - [20] U. Ellwanger, C. Hugonie, and A. M. Teixeira, Phys.Rept. **496**, 1 (2010), arXiv:0910.1785 [hep-ph].
 - [21] R. Barbieri, L. J. Hall, Y. Nomura, and V. S. Rychkov, Phys.Rev. **D75**, 035007 (2007), arXiv:hep-ph/0607332 [hep-ph].
 - [22] P. Batra, A. Delgado, D. E. Kaplan, and T. M. Tait, JHEP **0402**, 043 (2004), arXiv:hep-ph/0309149 [hep-ph].
 - [23] A. Brignole, J. Casas, J. Espinosa, and I. Navarro, Nucl.Phys. **B666**, 105 (2003), arXiv:hep-ph/0301121 [hep-ph].
 - [24] T. Goerdt, O. Y. Gnedin, B. Moore, J. Diemand, and J. Stadel, Mon.Not.Roy.Astron.Soc. **375**, 191 (2007), arXiv:astro-ph/0608495 [astro-ph].
 - [25] A. Arbey, M. Battaglia, A. Djouadi, F. Mahmoudi, and J. Quevillon, Phys.Lett. **B708**, 162 (2012), arXiv:1112.3028 [hep-ph].
 - [26] N. Polonsky and A. Pomarol, Phys.Rev.Lett. **73**, 2292 (1994), arXiv:hep-ph/9406224 [hep-ph].
 - [27] G. Giudice and A. Romanino, Nucl.Phys. **B699**, 65 (2004), arXiv:hep-ph/0406088 [hep-ph].
 - [28] G. Aad *et al.* (ATLAS), JHEP **1409**, 176 (2014), arXiv:1405.7875 [hep-ex].
 - [29] C. Collaboration (CMS), (2014).
 - [30] C. Stenge, G. Bertone, G. J. Besjes, S. Caron, R. Ruiz de Austri, A. Strubig, and R. Trotta, JHEP **09**, 081 (2014), arXiv:1405.0622 [hep-ph].
 - [31] K. J. de Vries (MasterCode), in *International Conference on High Energy Physics 2014 (ICHEP 2014) Valencia, Spain, July 2-9, 2014* (2014) arXiv:1410.6755 [hep-ph].
 - [32] K. J. de Vries *et al.*, (2015), arXiv:1504.03260 [hep-ph].
 - [33] E. A. Bagnaschi *et al.*, (2015), arXiv:1508.01173 [hep-ph].
 - [34] P. Grothaus, M. Lindner, and Y. Takanishi, JHEP **1307**, 094 (2013), arXiv:1207.4434 [hep-ph].
 - [35] C. Cheung, L. J. Hall, D. Pinner, and J. T. Ruderman, JHEP **1305**, 100 (2013), arXiv:1211.4873 [hep-ph].
 - [36] M. E. Cabrera, J. A. Casas, and R. Ruiz de Austri, JHEP **03**, 075 (2009), arXiv:0812.0536 [hep-ph].

- [37] R. Barbieri and G. Giudice, Nucl.Phys. **B306**, 63 (1988).
- [38] D. M. Ghilencea, Phys. Rev. **D89**, 095007 (2014), arXiv:1311.6144 [hep-ph].
- [39] S. S. AbdusSalam, B. C. Allanach, F. Quevedo, F. Feroz, and M. Hobson, Phys.Rev. **D81**, 095012 (2010), arXiv:0904.2548 [hep-ph].
- [40] S. S. AbdusSalam, Int. J. Mod. Phys. **A29**, 1450160 (2014), arXiv:1312.7830 [hep-ph].
- [41] S. S. AbdusSalam, C. P. Burgess, and F. Quevedo, JHEP **02**, 073 (2015), arXiv:1411.1663 [hep-ph].
- [42] J. D. Etienne Auge and J. T. T. Van, (2013).
- [43] W. Yao *et al.* (Particle Data Group), J.Phys. **G33**, 1 (2006).
- [44] K. Hagiwara, A. Martin, D. Nomura, and T. Teubner, Phys.Lett. **B649**, 173 (2007), arXiv:hep-ph/0611102 [hep-ph].
- [45] M. E. Cabrera, A. Casas, R. R. de Austri, and G. Bertone, (2013), arXiv:1311.7152 [hep-ph].
- [46] “The LEP Electroweak Working Group,” <http://lepewwg.web.cern.ch/LEPEWWG>.
- [47] Y. Amhis *et al.* (Heavy Flavor Averaging Group), (2012), arXiv:1207.1158 [hep-ex].
- [48] R. Aaij *et al.* (LHCb), Phys.Lett. **B709**, 177 (2012), arXiv:1112.4311 [hep-ex].
- [49] B. Aubert *et al.* (BaBar Collaboration), Phys.Rev.Lett. **100**, 021801 (2008), arXiv:0709.1698 [hep-ex].
- [50] M. Antonelli *et al.* (FlaviaNet Working Group on Kaon Decays), (2008), arXiv:0801.1817 [hep-ph].
- [51] R. Aaij *et al.* (LHCb Collaboration), Phys.Rev.Lett. **110**, 021801 (2013), arXiv:1211.2674 [hep-ex].
- [52] Y. Amhis *et al.* (Heavy Flavor Averaging Group (HFAG)), (2014), arXiv:1412.7515 [hep-ex].
- [53] T. Saito *et al.* (Belle), Phys. Rev. **D91**, 052004 (2015), arXiv:1411.7198 [hep-ex].
- [54] J. P. Lees *et al.* (BaBar), Phys. Rev. **D86**, 052012 (2012), arXiv:1207.2520 [hep-ex].
- [55] V. Khachatryan *et al.* (LHCb, CMS), Nature **522**, 68 (2015), arXiv:1411.4413 [hep-ex].
- [56] G. Aad *et al.* (ATLAS Collaboration), Phys.Lett. **B716**, 1 (2012), arXiv:1207.7214 [hep-ex].
- [57] S. Chatrchyan *et al.* (CMS Collaboration), Phys.Lett. **B716**, 30 (2012), arXiv:1207.7235 [hep-ex].
- [58] E. Aprile *et al.* (XENON100 Collaboration), Phys.Rev.Lett. **109**, 181301 (2012), arXiv:1207.5988 [astro-ph.CO].
- [59] P. Ade *et al.* (Planck), Astron.Astrophys. **571**, A16 (2014), arXiv:1303.5076 [astro-ph.CO].
- [60] G. Bertone, D. G. Cerdeno, M. Fornasa, R. R. de Austri, and R. Trotta, Phys.Rev. **D82**, 055008 (2010), arXiv:1005.4280 [hep-ph].
- [61] <http://lepewwg.web.cern.ch/LEPEWWG>.
- [62] Y. Amhis *et al.* (Heavy Flavor Averaging Group), (2012), arXiv:1207.1158 [hep-ex].
- [63] B. Aubert *et al.* (BABAR), (2008), arXiv:0808.1915 [hep-ex].
- [64] P. Ade *et al.* (Planck), Astron.Astrophys. **571**, A16 (2014), arXiv:1303.5076 [astro-ph.CO].
- [65] R. R. de Austri, R. Trotta, and L. Roszkowski, JHEP **0605**, 002 (2006), arXiv:hep-ph/0602028 [hep-ph].
- [66] E. Aprile *et al.* (XENON100), Phys.Rev.Lett. **109**, 181301 (2012), arXiv:1207.5988 [astro-ph.CO].
- [67] F. Feroz and M. P. Hobson, Mon. Not. Roy. Astron. Soc. **384**, 449 (2008), arXiv:0704.3704 [astro-ph].
- [68] F. Feroz, M. P. Hobson, and M. Bridges, Mon. Not. Roy. Astron. Soc. **398**, 1601 (2009), arXiv:0809.3437 [astro-ph].
- [69] B. Allanach, Comput.Phys.Comm. **143**, 305 (2002), arXiv:hep-ph/0104145 [hep-ph].
- [70] G. Belanger, F. Boudjema, A. Pukhov, and A. Semenov, Comput.Phys.Comm. **149**, 103 (2002), arXiv:hep-ph/0112278 [hep-ph].
- [71] P. Gondolo, J. Edsjo, L. Bergstrom, P. Ullio, and E. A. Baltz, , 318 (2000), arXiv:astro-ph/0012234 [astro-ph].
- [72] J. R. Ellis, K. A. Olive, and C. Savage, Phys.Rev. **D77**, 065026 (2008), arXiv:0801.3656 [hep-ph].
- [73] G. Degrandi, P. Gambino, and P. Slavich, Comput.Phys.Comm. **179**, 759 (2008), arXiv:0712.3265 [hep-ph].
- [74] F. Mahmoudi, Comput.Phys.Comm. **180**, 1579 (2009), arXiv:0808.3144 [hep-ph].
- [75] A. Sommerfeld, Annalen der Physik **403**, 257 (1931).
- [76] J. Hisano, S. Matsumoto, M. Nagai, O. Saito, and M. Senami, AIP Conf.Proc. **957**, 401 (2007).
- [77] T. R. Slatyer, JCAP **1002**, 028 (2010), arXiv:0910.5713 [hep-ph].
- [78] S. Cassel, J.Phys. **G37**, 105009 (2010), arXiv:0903.5307 [hep-ph].
- [79] R. Iengo, JHEP **0905**, 024 (2009), arXiv:0902.0688 [hep-ph].
- [80] L. Visinelli and P. Gondolo, (2010), arXiv:1007.2903 [hep-ph].
- [81] A. Hryczuk, R. Iengo, and P. Ullio, JHEP **1103**, 069 (2011), arXiv:1010.2172 [hep-ph].
- [82] A. Hryczuk, Phys.Lett. **B699**, 271 (2011), arXiv:1102.4295 [hep-ph].

- [83] T. Bringmann, *New J.Phys.* **11**, 105027 (2009), arXiv:0903.0189 [astro-ph.CO].
- [84] A. M. Green, S. Hofmann, and D. J. Schwarz, *Mon.Not.Roy.Astron.Soc.* **353**, L23 (2004), arXiv:astro-ph/0309621 [astro-ph].
- [85] A. M. Green and S. P. Goodwin, *Mon.Not.Roy.Astron.Soc.* **375**, 1111 (2007), arXiv:astro-ph/0604142 [astro-ph].
- [86] S. Hofmann, D. Schwarz, and H. Stoecker, , 45 (2002), arXiv:astro-ph/0211325 [astro-ph].
- [87] V. Berezhinsky, V. Dokuchaev, and Y. Eroshenko, *Phys.Rev.* **D68**, 103003 (2003), arXiv:astro-ph/0301551 [astro-ph].
- [88] N. Arkani-Hamed, A. Delgado, and G. Giudice, *Nucl.Phys.* **B741**, 108 (2006), arXiv:hep-ph/0601041 [hep-ph].
- [89] K. Griest and D. Seckel, *Phys.Rev.* **D43**, 3191 (1991).
- [90] “LHC SUSY Cross Section Working Group,” https://twiki.cern.ch/twiki/bin/view/LHCPhysics/SUSYCrossSections#SUSY_Cross_Sections_using_8_TeV.
- [91] T. Sjostrand, S. Mrenna, and P. Z. Skands, *JHEP* **0605**, 026 (2006), arXiv:hep-ph/0603175 [hep-ph].
- [92] T. Sjostrand, S. Mrenna, and P. Z. Skands, *Comput.Phys.Commun.* **178**, 852 (2008), arXiv:0710.3820 [hep-ph].
- [93] G. Aad *et al.* (ATLAS), (2015), arXiv:1507.04548 [hep-ex].
- [94] A. Djouadi, M. Muhlleitner, and M. Spira, *Acta Phys.Polon.* **B38**, 635 (2007), arXiv:hep-ph/0609292 [hep-ph].
- [95] G. Aad *et al.* (ATLAS), *JHEP* **1406**, 124 (2014), arXiv:1403.4853 [hep-ex].
- [96] G. Aad *et al.* (ATLAS), *JHEP* **1409**, 015 (2014), arXiv:1406.1122 [hep-ex].
- [97] G. Aad *et al.* (ATLAS), *Phys.Rev.* **D90**, 052008 (2014), arXiv:1407.0608 [hep-ex].
- [98] G. Aad *et al.* (ATLAS), *JHEP* **1410**, 24 (2014), arXiv:1407.0600 [hep-ex].
- [99] G. Aad *et al.* (ATLAS), *JHEP* **1405**, 071 (2014), arXiv:1403.5294 [hep-ex].
- [100] J. Edsjo, (1997), arXiv:hep-ph/9704384 [hep-ph].
- [101] G. Aad *et al.* (ATLAS), (2015), arXiv:1507.05525 [hep-ex].
- [102] P. Cushman, C. Galbiati, D. McKinsey, H. Robertson, T. Tait, *et al.*, (2013), arXiv:1310.8327 [hep-ex].
- [103] D. Mallin, D. Akerib, H. Araujo, X. Bai, S. Bedikian, *et al.*, (2011), arXiv:1110.0103 [astro-ph.IM].
- [104] D. Akerib *et al.* (LUX Collaboration), (2013), arXiv:1310.8214 [astro-ph.CO].
- [105] S. R. Golwala, (2000).
- [106] P. Junnarkar and A. Walker-Loud, *Phys.Rev.* **D87**, 114510 (2013), arXiv:1301.1114 [hep-lat].
- [107] A. Crivellin, M. Hoferichter, and M. Procura, *Phys. Rev.* **D89**, 054021 (2014), arXiv:1312.4951 [hep-ph].
- [108] A. Crivellin, M. Hoferichter, M. Procura, and L. C. Tunstall, *JHEP* **07**, 129 (2015), arXiv:1503.03478 [hep-ph].
- [109] R. J. Hill and M. P. Solon, *Phys.Rev.Lett.* **112**, 211602 (2014), arXiv:1309.4092 [hep-ph].
- [110] R. J. Hill and M. P. Solon, *Phys.Rev.* **D91**, 043505 (2015), arXiv:1409.8290 [hep-ph].
- [111] V. Springel, J. Wang, M. Vogelsberger, A. Ludlow, A. Jenkins, *et al.*, *Mon.Not.Roy.Astron.Soc.* **391**, 1685 (2008), arXiv:0809.0898 [astro-ph].
- [112] J. Diemand, M. Kuhlen, and P. Madau, *Astrophys.J.* **667**, 859 (2007), arXiv:astro-ph/0703337 [astro-ph].
- [113] J. Diemand, M. Kuhlen, and P. Madau, *Astrophys.J.* **657**, 262 (2007), arXiv:astro-ph/0611370 [astro-ph].
- [114] J. F. Navarro, C. S. Frenk, and S. D. White, *Mon.Not.Roy.Astron.Soc.* **275**, 720 (1995), arXiv:astro-ph/9408069 [astro-ph].
- [115] S. Ando, *Phys.Rev.* **D80**, 023520 (2009), arXiv:0903.4685 [astro-ph.CO].
- [116] T. Cohen, M. Lisanti, A. Pierce, and T. R. Slatyer, *JCAP* **1310**, 061 (2013), arXiv:1307.4082.
- [117] J. Fan and M. Reece, *JHEP* **1310**, 124 (2013), arXiv:1307.4400 [hep-ph].
- [118] A. Hryczuk, I. Cholis, R. Iengo, M. Tavakoli, and P. Ullio, (2014), arXiv:1401.6212 [astro-ph.HE].
- [119] M. E. C. Catalan, S. Ando, C. Weniger, and F. Zandanel, (2015), arXiv:1503.00599 [hep-ph].
- [120] S. Ambrosanio and B. Mele, *Phys.Rev.* **D55**, 1399 (1997), arXiv:hep-ph/9609212 [hep-ph].
- [121] M. A. Diaz, B. Panes, and P. Urrejola, *Eur.Phys.J.* **C67**, 181 (2010), arXiv:0910.1554 [hep-ph].
- [122] N. Desai, J. Ellis, F. Luo, and J. Marrouche, *Phys.Rev.* **D90**, 055031 (2014), arXiv:1404.5061 [hep-ph].
- [123] S. P. Martin, *Phys.Rev.* **D78**, 055019 (2008), arXiv:0807.2820 [hep-ph].
- [124] S. Bornhauser, M. Drees, S. Grab, and J. Kim, *Phys.Rev.* **D83**, 035008 (2011), arXiv:1011.5508

- [125] [hep-ph].
A. Delgado, G. F. Giudice, G. Isidori, M. Pierini, and A. Strumia, Eur.Phys.J. **C73**, 2370 (2013), arXiv:1212.6847 [hep-ph].